Linear theory and applications in AFM

Tuza Adeyemi Olukan
Sergio Santos
Lamia Sami Elsherbiny
Matteo Chiesa

Oscillations – Linear theory and applications in AFM

Authors

Tuza Adeyemi Olukan[1]
Sergio Santos
Lamia Sami Elsherbiny[2]
Matteo Chiesa[1,2]

Corresponding authors:

Affiliations:

1. ARC-Arctic Centre for Sustainable Energy, Department of Physics and Technology, UiT The Arctic University of Norway, 9010 Tromsø, Norway
2. Laboratory for Energy and Nano Science, Masdar Campus, Khalifa University, Abu Dhabi, United Arab Emirates

Design and layout: Maritsa Kissamitaki

Contents

Glossary

m	mass
z	position of the tip relative to the cantilever
d	tip-sample distance
t	time
Q	Q factor
ω_0	natural frequency
k	spring constant
F_0	magnitude of drive force
ϕ	phase shift
F_{ts}	tip-sample (surface) force
$\ddot{z}$	acceleration
$\dot{z}$	velocity
T	period
W	work
U	potential energy
KE	kinetic energy
E_T	total energy
E_{avg}	average energy
<E>	average energy
δ	deformation
P_{dis}	power dissipation
A	amplitude
A_0	free amplitude
W_D	work done by the drive
V	virial
E_{dis}	energy dissipation
ω_r	resonance frequency
ω_{eff}	effective resonance frequency
ω_0'	effective resonance frequency

Introduction

The theory of oscillations can be studied from a mathematical point of view in terms of differential equations. The differential equation is written and then the solution or solutions worked out and mathematically analysed. Provided physical, economic, social, or other phenomena can be modelled in terms of equivalent differential equations, the solutions and results are applicable to all phenomena all the same. On the other hand, it is sometimes easier to learn a topic by having an experimental topic in mind. It is otherwise maybe surprising that a large body of phenomena in many fields of application will be easily understood if the equations are understood for a given case. The experimental analysis that forms the basis of this book is cantilever dynamics in dynamic atomic force microscopy (AFM). In a nutshell, the motion of the cantilever in dynamic AFM can be approximated to a perturbed driven oscillator. The generality of the analysis presented here can be confirmed by noting that much of what is covered in this book, particularly when dealing with the linear equation in section 1, is similar to what is covered in generic expositions such as that by Tipler and Mosca[1] or the Feynman's lectures on physics[2]. Maybe the main advantage of this exposition is that the linear and nonlinear theories of oscillators, particularly phenomena that can be reduced to the analysis of a point-mass on a spring, are discussed in detail and differences in terminology that could lead to doubt, clarified. This means that this book can be used as a textbook to teach oscillation theory with a focus on applications. This is possible because oscillations are present generally in physics, engineering, biology, economics, sociology and so on. In summary, all phenomena dealing with oscillations can be reduced, to a first approximation, to a restoring parameter, i.e., force in mechanics, following Hooke's law.

Since the AFM field is a niche in science, the general theory of oscillation does not cover the particularities of the field. This book covers such particularities. Thus, the book can be used as an introduction to dynamic AFM and oscillation theory that covers the terminology required to understand dynamic AFM. On the other hand, the ubiquity and generality of oscillation theory ensures that the book can also be used as a general introduction to oscillation theory at an undergraduate level. There is also advanced material, particularly in the second section of the book where nonlinearities are covered.

For the sake of transnationality, standard terminology is employed throughout when possible, especially in the first section (Book 1). The first section is based on the standard linear differential equations. The second section is based on non-linear theory and covers advancements in dynamic FM over the past three decades (1990s – 2022). Both sections are complimentary and exploit standard terminology in oscillation theory when possible.

The first section can be supplemented with the chapter on oscillations by Tipler and Mosca[1] and with Feynman's lectures on physics, volume 1, chapters 21 to 23. These two textbooks use standard terminology, even if not necessarily the same. Examples are drawn here from both texts and analogies also exploited.

The second section is mathematically more advanced since it discusses nonlinear theory. The second section is highly geared towards applications in AFM, but this does not mean that the discussion lacks generality. Rather, the nonlinear theory presented here is highly general and translational. The second section can be supplemented by following Raman's course on dynamic AFM. His course is available online[3]. There are another two important resources to supplement the second section. First, the thesis of Carlos Álvarez Amo, also available online[4]. Second, a varied set of papers that are referenced throughout the text.

1. Oscillations, linear theory, and applications in AFM

1.1 Oscillations in general

The oscillation of systems is a general phenomenon. A system oscillates if there is motion of the system around a neutral position. In dynamic atomic force microscopy (AFM) the physical system consists of a microcantilever which is made to oscillate around its position of equilibrium near a surface. A very sharp tip at the end of the cantilever periodically interacts with the surface via nanoscale forces. If the AFM cantilever vibrates far from the surface, i.e., ~ 10- 10^3 nm away from the surface, in a vacuum, in air or in liquids, and provided the amplitude of oscillation is sufficiently small, i.e., ~ 1- 10^2 nm, the oscillation is approximately linear, and the linear theory of oscillations applies. When the tip interacts closer to the surface, a nonlinear term, i.e., the tip-sample force F_{ts}, is introduced and the nonlinear theory applies.

Typical systems that oscillate are a pendulum or waves deep in the ocean, i.e. water moves up and down around a neutral position. Importantly, the physics of vibrations, or oscillations, of mechanical systems can be extended to the oscillations of dynamic systems in fields ranging from atomic and molecular physics[5-7], biological systems[8-11], automobile mechanics[12], and economics[13]. Even the human body has a multitude of sensory organs responding to vibrations[10-11]. In this respect, and while this book is concerned with oscillation theory based on the mass-point-spring model applied to AFM theory and experiment, the results are valid for any such system that can be reasonably well modelled as a point mass on a spring. The main mathematical trick consists in finding effective values for the parameters of the mathematical model. Provided such effective values can be found and provide the system can be reasonably well modelled as a mass-point-spring, the results are mathematically equivalent to the dynamics of oscillation of any general system. If these prerequisites are met, the oscillations of small, large, or even complex systems can be understood from the expressions, theory and experiments discussed here. The first chapters deal with the linear theory, but this theory is shown to be crucial when considering nonlinear behaviour. It will be shown in section 2 that the linear theory plays a very important role in the development of the mathematical formalism and interpretation of nonlinear behaviour. The nonlinear discussion treats oscillations affected by any nonlinear interaction, that is, by any general interaction including those emerging from conservative and dissipative phenomena. Finally, the transient response will not be discussed here in details since the focus will be the steady state response, i.e., the system oscillating in equilibrium.

An AFM microcantilever is shown in Fig. 1a. In Fig. 1b we find a simplified schematic of the microcantilever on the basis of which a rheological model can be derived (Fig. 2). A similar schematic is provided in Fig. 1 by Lozano and Garcia in their 2009 paper. This schematic (Fig. 1b and Eq. 1) aims to provide an accurate description of the dynamic behaviour of the microcantilever. It is important when dealing with phenomena to draw such schematics since these allow deriving the main parameters in the model by visual inspection and by using simple algebra. Constraints can thus be found. From Fig. 1b the following geometric[14] parameters can be defined

z: tip position in the vertical axis,

z_c: cantilever equilibrium distance,

d: tip-sample distance,

x: cantilever position in the x axis,

L: length of the cantilever

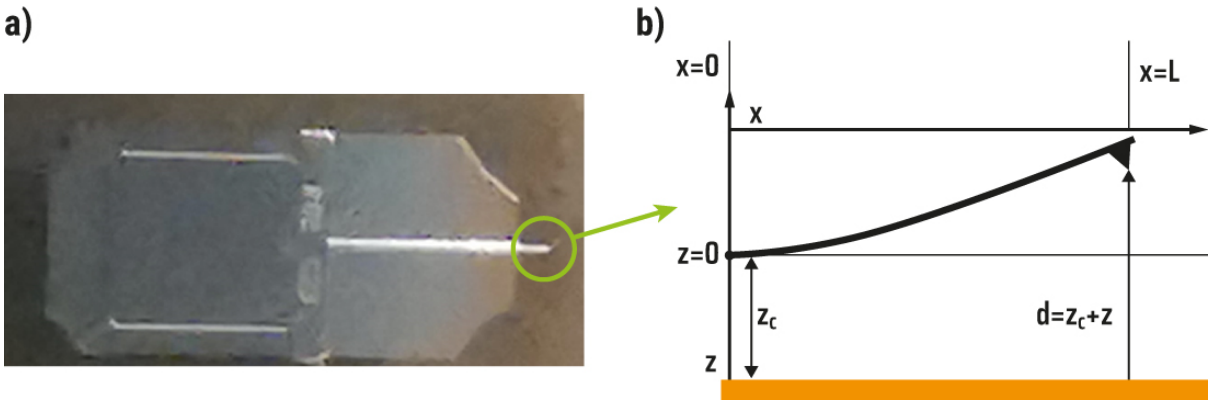

Figure 1. a) Photo of a real AFM microcantilever and the cantilever folder. The microcantilevers is some 100µm in length (circle). b) Simplified schematic of the microcantilever that allows to model the system by exploiting beam theory[14-16].

1.2 Continuous and point-mass model descriptions of the cantilever-tip system

The motion of a system like that shown in Fig. 1 must be simplified and described in terms of a model that is both 1) relatively easy to understand from a physical point of view and 2) later allows quantifying the relevant parameters in a given experiment. As it turns out, this step is crucial to investigate oscillations and it is many times possible to reduce the motion of many dynamic systems to the spring-mass model (Fig. 2). Several groups in the AFM community[17-19] have shown that the well-known Euler–Bernoulli beam theory[15-16] leads to the standard equation of the driven oscillator. For example, our group employed such theory to understand the implications of directly and indirectly driving the cantilever. In these papers the Euler–Bernoulli beam equation that governs the dynamics of a rectangular beam (Eq. 1) [20-21] is described in terms of the relevant experimental AFM parameters. The reader can refer to any of the above papers to understand how the motion of the AFM cantilever, in particular the tip's position at x=L, can be modelled as the standard spring-mass model. For example, equations 27 and 33 by Lozano and Garcia[17], treat the Euler–Bernoulli beam equation, their equation 18, as follows

$$EI\frac{\partial}{\partial x^4}\left[w(x,t)+a_1\frac{\partial w(x,t)}{\partial t}\right]+\rho bh\frac{\partial^2 w(x,t)}{\partial t^2} = -a_0\frac{\partial w(x,t)}{\partial t}+\delta(x-L)[F_{\text{exc}}(t)+F_{ts}(d)] \qquad \text{Eq. 1}$$

where E is the cantilever's Young's modulus, I is the area moment of inertia, a_1 is the internal damping coefficient, ρ is the mass density, b, h, and L are, respectively, the width, height, and length of the cantilever, a_0 is the hydrodynamic damping, w(x,t) is the time-dependent vertical displacement of the differential beam's element placed at the x position, $F_{exc}(t)$ is the excitation force and F_{ts} is the tip-sample force (compare with Fig. 1b).

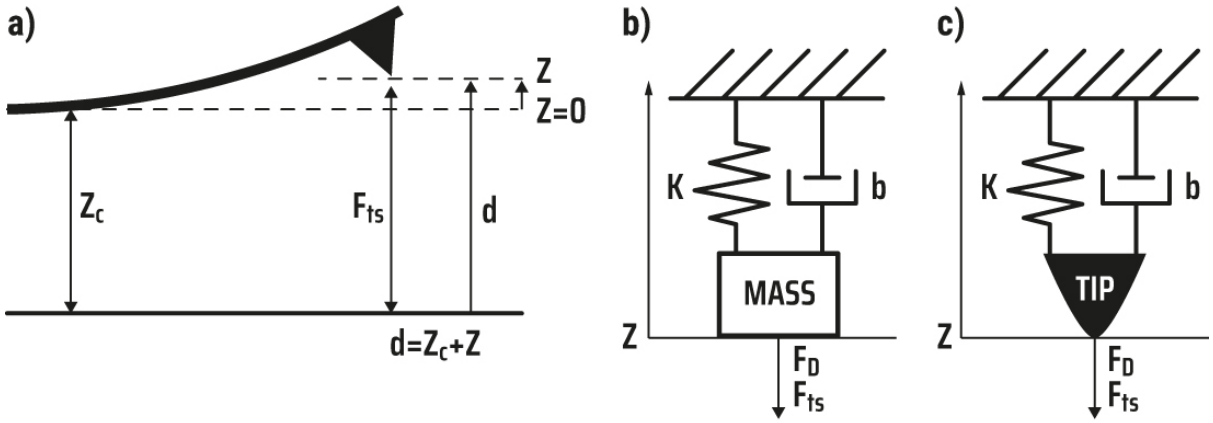

Figure 2. a) Schematic of an AFM cantilever from which geometrical constraints can be derived. b) and c) Rheological models of the tip' motion. Both models are mathematically equivalent but the illustration in c) showcases that the motion is discussed in terms of the tip.

The expression in Eq. 1 can be reduced to the standard differential equation describing the motion of a driven oscillator modelled as a mass and a spring (Eqs. 2-4). For this reason, understanding the standard linear theory is critical in order to understand AFM cantilever dynamics. There are many textbooks where the linear theory is described at the undergraduate level. For example the Tipler and Mosca's chapter on oscillations[1] or Feynman's lectures on physics, volume 1, chapters 21 to 23. The first part of this book is dedicated to the linear theory, and it is partly based on the two texts above with a focus on experiments in AFM. The second part is dedicated to the nonlinear theory, but it is still general.

To show that Eq. 1 is equivalent to a set of anharmonic differential equations, standard vibration theory can be exploited. In particular, Eq. 1 can be reduced to the following expression[17, 21]

$$\ddot{Y}_m(t) + \frac{\omega_m}{Q_m}\dot{Y}_m(t) + \omega_m^2 Y_m(t) = \frac{F_m(t)}{m_m}, m(subscript) = 1,2,\ldots \qquad \text{Eq. 2}$$

The notation in Eq. 2 is that of Lozano and García[17] (refer to their equations 27 and 33). While Lozano and García have used n as a subscript, we have used m (subscript) to refer to the set of modes because n is reserved for harmonics and because m typically stands for mode, i.e., note that Lozano and Garcia write n where we write m. $Y_m(t)$ is the time-dependent function of each eigen-mode. In Eq. 2 m is the effective mass, Q is the effective quality factor, ω are the natural frequencies, and F(t) are the external forces.

Finally, it can be shown that the expression in Eq. 2 can be reduced to Eq.3 at x=L where

$$\ddot{z}_m(t) + \frac{\omega_m}{Q_m}\dot{z}_m(t) + \omega_m^2 z_m(t) = \frac{F_{\text{exc}}(t) + F_{ts}(d)}{\text{m}}, m(subscript) = 1,2,\ldots \qquad \text{Eq. 3}$$

and where z(t) is the modal projection of the tip motion. Eq. 3 is a set of equations where we obtain one equation for each eigen mode m. In the rest of the chapter on linear theory only m=1 will be considered but most of the derivations are valid for the higher modes. The textbooks by Mosca and Tipler and Feynman analyse such expressions albeit F_{ts}=0 in their analysis since only linear forces are considered. In summary, this book is dedicated to the analysis of the expressions in Eq. 3 with a focus on AFM experiments, while the theory and considerations are, for the most part, general for other systems.

Since Eq. 1 is equivalent to the standard driven oscillator model typically discussed in textbooks, the standard rheological model in Fig. 2 applies. This mens that the description and the analysis of this model are equivalent to the analysis of AFM theory. Such model can be derived from the geometry of the AFM set up as shown in Fig. 2a. All the parameters in Fig. 2 have been already defined.

1.3 Simple harmonic motion

If only the first mode of oscillation is considered, the full equation of motion governing the dynamics of the cantilever at the tip-sample junction can be reduced to[22-28]

$$m\ddot{z} + b\dot{z} + kz = F_D + F_{ts}$$

$$m\ddot{z} + b\dot{z} + kz = F_{exc} + F_{ts}$$

$$m\ddot{z} + b\dot{z} + kz = F_0 \cos\ \omega t + F_{ts} \qquad \text{Eq. 4}$$

where the first term is the net force, i.e., mass times acceleration, from Newton's laws of motion, the second term stands for viscous dissipation, the third term is the restoring force of the spring, and the terms on the right are the drive force $F_D(t) \equiv F_0\cos(\omega t)$ and the tip sample interaction F_{ts}. We have written the drive force in many ways in Eq. 4 because the reader must pay attention to the definition given in each text. In particular, sometimes F_D is defined[29] as F_0 or as the amplitude[23, 30] of the drive A_D. The terminology is equivalent to that used by Tipler and Mosca in their chapter on oscillation under the subtitle resonance with the only main difference being that the last term is missing. In Feynman's lectures on physics, in chapter 23 - Feynman's equation is written as Eq. 23.6 - but Feynman writes c rather than b. In order to avoid confusions we note that Lozano and Garcia write F_d as $F_{exc}(t)$ as shown in Eqs. 1 and 3. The rest of chapters devoted to the linear theory deal with the analysis of Eq. 4 term by term with the exception of F_{ts}.

The first thing to note is that the rheological schematic in Figs. 2b and 2c can be used to derive Eq. 4 by applying Newton's laws.

Next Eq. 4 is reduced to two terms only giving

$$m\ddot{z} = -kz \qquad \text{Eq. 5}$$

where all the terms in Eq. 5 have been defined. That the terms have been formally defined does not mean that m or k are known in advance in a given experiment. Rather it is under the process known as calibration that the values of m and k will have to be found[31-32]. This is standard routine in AFM, but also a routine that should be followed whenever dealing with oscillations modelled via Eq. 4. It is the mathematical exploration of Eq. 4 that will provide the tools to physically calibrate these parameters, i.e., to find effective values for these terms. Here

effective simply means that the system will behave "as if" it had mass m and spring constant k. That is, since m only represents the effective mass of the system, m does not refer to the actual mass of the cantilever. Using experimental data to determine the value of m is what ensures the model's consistency. The same can be said about the rest of parameters involved in Eq. 4. The rheological model for Eq. 5 is shown in Fig. 3.

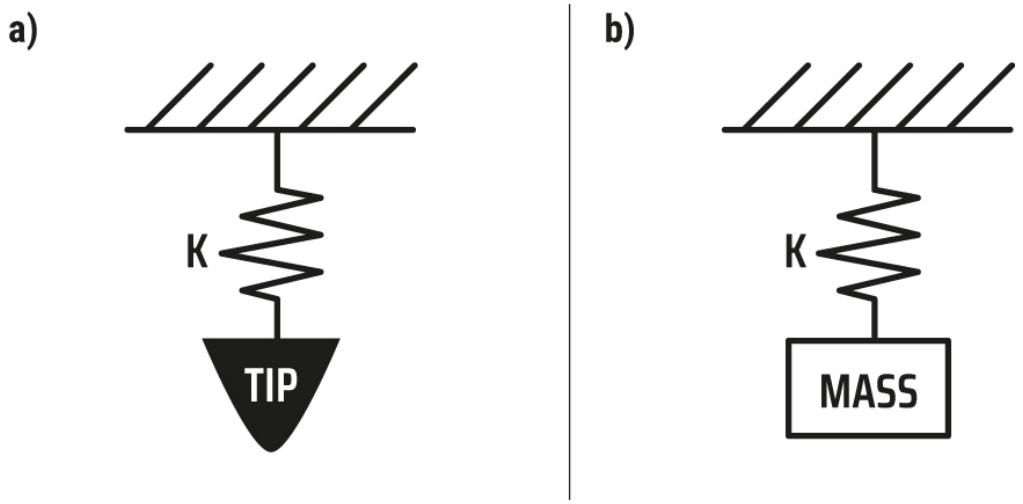

Figure 3. a) and b) Rheological models of the tip' motion. Both models are mathematically equivalent but the illustration in a) showcases that the motion is discussed in terms of the tip.

The exploration of Eq. 5 provides an insight into the physical meaning of the terms in the equation. Otherwise Eq. 5 is typically known as the equation describing simple harmonic motion. Considering Eq. 5 alone, the only force acting on the mass is the restoring force

$$F = -kz$$

$$m\ddot{z} = -kz \qquad \text{Eq. 6}$$

Eq. 6 is the Newton's equation for representing the model in Fig. 3. The physical meaning of such force is that whenever the object of mass m is displaced from its equilibrium position z=0, the force tends to bring it back to z=0. For this reason the force in Eq. 6 is typically termed "restoring force", i.e., it tends to restore the mass to its equilibrium position. This is the typical behaviour of a spring. Spring might further act on extension or compression, but they always tend to restore the equilibrium position. Provided the restoring force is proportional to the

displacement, the restoring force is linear as shown in Eq. 6. At this point is worth clarifying that under this model (Figs. 2-3) the object is an ideal point of mass m. This ideal point can represent any physical system of finite size.

It is essential to understand how the "natural frequency", ω_0, which is an angular frequency given in radians, is derived from this equation. The meaning of "natural" will be discussed as the analysis proceeds.

The position of the point of mass m is determined as z and the behaviour of the mass is parametrized through Eqs. 7-9.

$$z = A\cos(\omega t + \phi) \quad \text{Eq. 7}$$

$$\ddot{z} = -A\omega^2\cos(\omega t + \phi) \quad \text{Eq. 8}$$

$$\ddot{z} = -\frac{k}{m}z \quad \text{Eq. 9}$$

where A is the amplitude of oscillation and where the phase (shift) ϕ depends on where t=0 is defined.

In short, Eqs. 7-9 represent the solution of Eq. 5 as confirmed by substitution. Inserting Eqs. 7 and 8 into Eq. 5

$$-mA\omega^2\cos(\omega t + \phi) = -kA\cos(\omega t + \phi) \quad \text{Eq. 10}$$

$$-m\omega^2 = -k \quad \text{Eq. 11}$$

where the above are solutions provided the identity below is true

$$\omega^2 \equiv \frac{k}{m} \quad \text{Eq. 12}$$

Eq. 12 is the first important result since k and m can now be related to a parameter that can be experimentally measured, namely, the angular frequency at which the system will oscillate. The above identity is employed to define the natural frequency of oscillation.

$$\omega^2 = \frac{k}{m} \equiv \omega_0^2 \qquad \text{Eq. 13}$$

The frequency f in Hertz is given as usual

$$f_0 = \frac{\omega_0}{2\pi} \qquad \text{Eq. 14}$$

The spring constant is thus related to the mass and the angular frequency as follows

$$\omega_0 = \sqrt{k/m} \qquad \text{Eq. 15}$$

Eq.15 is the expression obtained when there is no dissipative term. This indicates that when the system resonates under the influence of no other force, for instance, in a high vacuum, a mass would move up and down sinusoidally at its natural frequency as given by Eqs. 12-15 above. The definition of the natural frequency further shows that it is given by conservative forces alone. This is because -kz is a conservative force.

The main result of the analysis in this section is that

1. When the only force on the mass is the restoring force, the tendency is to oscillate sinusoidally at frequency f_0 or ω_0.

2. The frequency of oscillation is termed “natural frequency” and it is determined by the effective mass m and the effective spring constant k.

3. Importantly, if there is nothing that disturbs the motion of the system, the mass will always remain in equilibrium.

When the mass moves outside equilibrium z=0 there is sinusoidal motion as described by Eq. 7. The description of such motion is left for the next chapters. It is also possible to understand the concepts of potential energy and kinetic energy from Eq. 5 alone, but such analysis is also left for the next chapters (chapter 1.5).

1.4 Damped oscillations

In this section, there are several objectives.

1. To extend the analysis to the situation where there is damping or dissipation. In particular we will deal with standard viscous damping. Viscous damping can be understood as friction within a medium, i.e., it opposes the motion and therefore has a tendency to stop the body[33].

2. To investigate the effects of dissipation. The addition of viscosity has two important effects. First it displaces the point of maximum amplitude. This implies that the system will now resonate at $\omega_r \neq \omega_0$, i.e., there is maximum amplitude at a frequency different to ω_0. Second, the system will respond with significant values of amplitude A at a range of frequencies around ω_r.

In short, the aim is to relate the frequency of resonance ω_r to the natural frequency ω_0 when there is viscous dissipation, such as air or liquids. In AFM, viscosity is present in air environments due to friction with air while in liquid environments there is friction du to the liquid. The natural frequency is related to the natural period T as shown in Eq. 16.

$$f_0 = \frac{1}{T_0} = \frac{1}{\frac{2\pi}{\omega_0}} = \frac{\omega_0}{2\pi} \equiv \frac{1}{2\pi}\sqrt{\frac{k}{m}} \qquad \text{Eq.16}$$

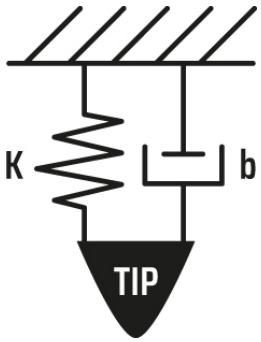

Figure 4. Rheological models of the tip' motion in the presence of viscosity.

To find a relationship between the resonance frequency and the natural frequency we begin with Eq. 17. This equation is derived from the rheological model shown in Fig. 4. This simplified model is also discussed in detail in standard textbooks, for example by Tipler and Mosca and in Feynman's lectures.

$$m\ddot{z} + b\dot{z} + kz = 0 \qquad \text{Eq.17}$$

First, the term b is sometimes written in terms of Q where Q is defined as

$$\gamma = \frac{\omega_0}{Q} \qquad \text{Eq.18}$$

and

$$b = m\frac{\omega_0}{Q} \equiv m\gamma \qquad \text{Eq.19}$$

It is the task of this chapter to go through the derivation and physical interpretation of Eqs. 18 and 19. In AFM the typical parameters that are calibrated during every experiment and routinely are the spring constant k, the resonant frequency ω_r and Q. Through these expressions the equation of motion Eq. 17 can be written in the following equivalent forms

$$\frac{k}{\omega_0^2}\ddot{z} + \frac{k}{\omega_0 Q}\dot{z} + kz = 0 \qquad \text{Eq. 20}$$

$$m\frac{d^2z}{dt^2} + \frac{m\omega_0}{Q}\frac{dz}{dt} + kz = 0 \qquad \text{Eq. 21}$$

$$\ddot{z} + \frac{b}{m}\,\dot{z} + \omega_0^2 z = 0 \qquad \text{Eq. 22}$$

Eqs. 17 and 20-22 are mathematically equivalent and exploit the relationships in Eqs. 12, 18 and 19. As the analysis of the linear system proceeds, further relationships are obtained, and these are incorporated into the theory. For this reason it is important to go through the full analysis.

In order to find a solution to Eq. 22 the following solution is proposed

$$z = Be^{i\omega t} \equiv z + iy \qquad \text{Eq. 23}$$

Since the equation of motion is linear, it follows that if $z = x + iy$ is a solution of Eq. 17 so are x and y.

Time derivatives produce the following result

$$z = Be^{i\omega t} \qquad \text{Eq. 24}$$

$$\dot{z} = i\omega Be^{i\omega t} \qquad \text{Eq. 25}$$

$$\ddot{z} = -\omega^2 Be^{i\omega t} \qquad \text{Eq. 26}$$

Substituting into Eq. 17,

$$-\omega^2 Be^{i\omega t} + \frac{b}{m}\, i\omega Be^{i\omega t} + \omega_0^2\, Be^{i\omega t} = 0 \qquad \text{Eq. 27}$$

Dividing by $Be^{i\omega t}$ results in the following expression

$$-\omega^2 - \frac{b}{m}\,i\omega + \omega_0^2 = 0 \qquad \text{Eq.28}$$

Now we have an equation that is quadratic in terms of ω. The equation is telling us that the system will resonate at $\omega \equiv \omega_r$ where the maximum value of A will be found at ω_r. This is a consequence of the presence of viscous damping, i.e., of the second term in Eq. 17. Since Eq. 28 contains ω_0, this solution provides a method to relate ω_r to ω_0 provided a solution ω is found.

Solving Eq. 28,

$$\omega^2 + \frac{ib\omega}{m} - \omega_0^2 = 0$$

$$\omega = \frac{ib}{2m} \pm \frac{1}{2}\sqrt{\left(\frac{ib}{m}\right)^2 + 4\omega_0^2}$$

$$\omega = \frac{b}{2m}i \;\; \pm \omega_0\sqrt{1 - \left(\frac{b}{2m\omega_0}\right)^2} \qquad \text{Eq. 29}$$

From linearity it follows that Eq. 29 contains all the solutions to Eq. 17 in

$$\omega = x + iy$$

This means that both x and y are solutions. Thus, the following is a solution ($\omega_r \equiv y$) to Eq. 17

$$\omega_r = \omega_0\sqrt{1 - \left(\frac{b}{2m\omega_0}\right)^2} = \omega_0\sqrt{1 - \frac{1}{4Q^2}} \qquad \text{Eq. 30}$$

Equation 30 explains that the resonance frequency will decrease with increasing dissipation b or decreasing Q. Only in the limit $Q \to \infty$ $\omega_r = \omega_0$. This is equivalent to saying b=0.

In AFM, frequency sweeps are taken to determine ω_r. Such frequency sweeps are taken high above the surface, i.e., $z_c \sim \mu m$. This means that taking a frequency sweep near the surface or

far from the surface will result in different values of ω_r if dissipation, i.e., b or Q, varies as a function of proximity to the surface. In other words, the result in Eq. 30 allows determining viscosity as a function of cantilever-surface proximity based on the shift from ω_0. The closer ω_r to ω_0 the less viscosity. Viscosity commonly increases as one approaches the surface. Consequently, one should observe a lower resonance frequency, that is, the peak in amplitude A should be found at lower frequencies, the closer the cantilever is brought to the surface. A standard frequency sweep performed with a cypher AFM is shown in Fig. 5.

In such sweep the amplitude A is shown for each value of ω from $0 < f < 400$ kHz (approx.). The idea is to get the value ω_r where ω_r is defined when the amplitude is reaches its maximum value. For values of Q that are relatively large, i.e., ~ 10, 100, $\omega_r \approx \omega_0$ as observed by inspecting of Eq. 30. For example, for Q=100 and $f_0 = \omega_0/2\pi$= 100 kHz, f_r = 99.999 kHz which is a 0.1% shift in frequency.

In ultra-high vacuum, typical values of Q are ~ 10000. In air environments Q ~ 100 and in liquid environments we experimentally find that Q ~ 1-10. In Fig. 5 there are several main peaks. The first peak corresponds to the resonance of the first mode while the second corresponds to the resonance of the second mode. The peak of the third mode is also observed near 1MHz. The other peaks in Fig. 5 are due to noise. This can be experimentally confirmed by exploring the graph with AFM software, but it has not been shown here. Physically, the cantilever will move very differently when resonating near the first and second modes. In Fig. 6 the typical behaviour of modes 1 and 2 is illustrated.

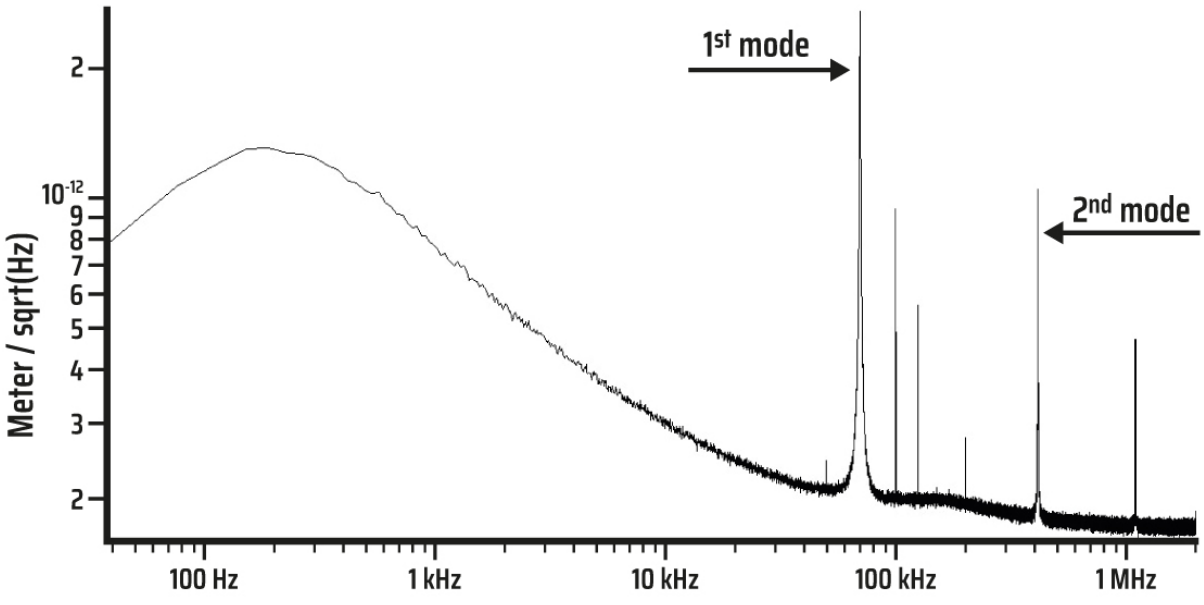

Figure 5. Standard frequency sweep for an AFM cantilever.

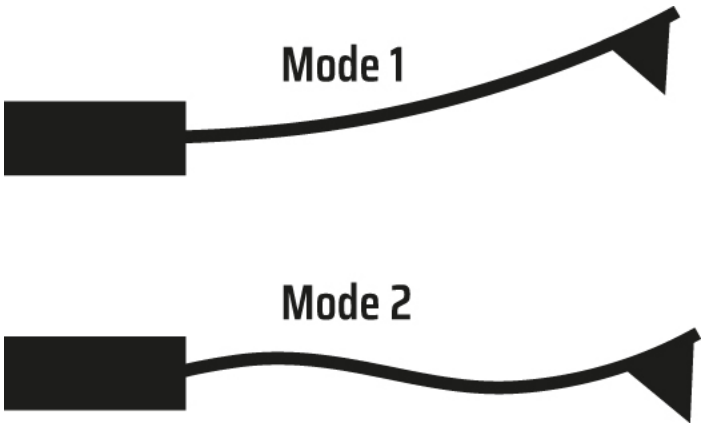

Figure 6. Illustration of the first two modes of a cantilever.

1.5 Relationship between stored energy and kinetic energy

This section covers the relationship between total stored energy E, potential energy U and kinetic energy KE through the analysis of the expression of simple harmonic motion. It is typical in textbooks to describe the relationship between stored energy and kinetic energy right after discussion of Eq. 5, that is, after the equation describing simple harmonic motion. See for example Tipler and Mosca's discussion on oscillations or the discussion provided by Feynman in his lectures. This is because if there is dissipation and no energy enters the system, for example by driving it with an external force F_d, the amplitude A will eventually reach 0, i.e., the system will stop. The rheological model describing Eq. 5 is shown again as Fig. 7 with the addition of an oscillatory sketch of amplitude A, i.e., $z=A\cos(\omega_0 t+\phi)$. The period of oscillation T is simply

$$T_0 = \frac{1}{f_0} \qquad \text{Eq. 31}$$

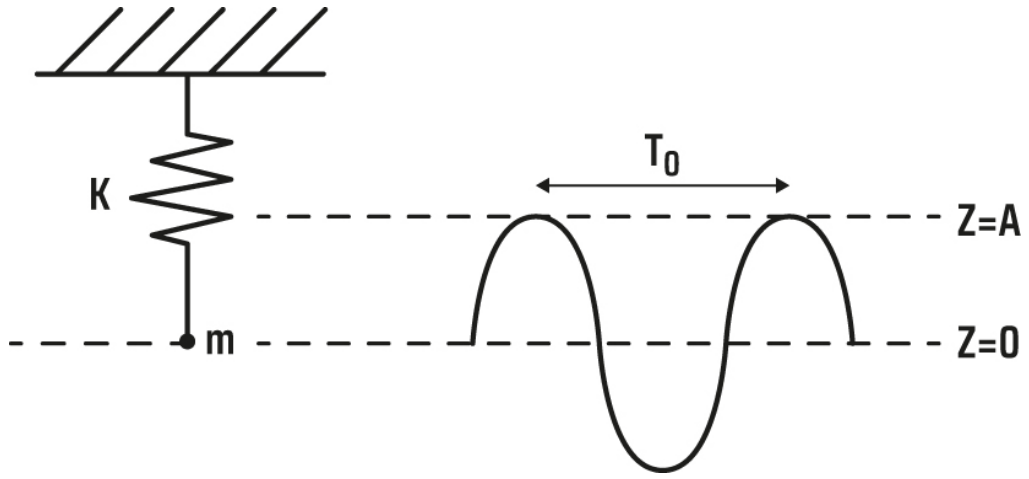

Figure 7. A rheological model describing Eq. 5 is shown again and oscillatory sketch of amplitude A and period T_0.

If there is no drive, in order to reach the amplitude A the spring must be extended to z=A. Then, it will oscillate with amplitude A. Since there is no dissipation, the energy stored at z=A and $\dot{z} = 0$ will remain in the system with time, i.e., dE/dt=0.

The total energy of the system is the sum of the potential energy and the kinetic energy. Using hook's law, the instantaneous potential energy stored in the spring as a function of time can be found as follows

$$F = -kz$$

$$dW = F \cdot dz \equiv du$$

$$W \equiv U = \int_{z_1}^{z_2} kzdz$$

$$W \equiv \Delta U = \frac{1}{2}kz_2^2 - \frac{1}{2}kz_1^2$$

$$U = \frac{1}{2}kz^2 + C \qquad \text{Eq. 32}$$

where dW is the differential of work done by the restoring force per differential displacement dz, the total work done from $z=z_1$ to $z=z_2$ is W which can be identified as the difference in potential energy ΔU from $z=z_1$ to $z=z_2$. The stored energy in the spring U is therefore arbitrarily defined. If the displacement occurs from z=0 to $z=z\equiv A$, then, as measured frm z=0 (U=0),

$$U_0 = \frac{1}{2}kA^2 \qquad \text{Eq. 33}$$

where the zero potential energy is also arbitrarily defined at z=0. For any arbitrary defined potential energy

$$U = \frac{1}{2}kz^2 + C \qquad \text{Eq. 34}$$

where the zero potential energy is arbitrarily as C at z=0. Typically C=0. The arbitrariness of defining U=C=0 at z=0 is due to the fact that only differences in potential energy are physically meaningful and it is useful to define potential energy in terms of the range of motion, i.e., range in z is 2A where $-A \leq z \leq A$. Furthermore, that the potential energy is zero when -kz=0 is also useful. Substituting Eq. 7 into Eq. 34

$$z = Acos(\omega t + \phi)$$

$$U = \frac{1}{2}kA^2\cos^2(\omega t + \phi) \qquad \text{Eq. 35}$$

Eq. 35 defines the instantaneous potential energy as a function of position z and z=z(t). The kinetic energy KE can be expressed as follows,

$$\dot{z} = -\omega A sin(\omega t + \phi)$$

$$KE = \frac{1}{2}mv^2 = \frac{1}{2}m\dot{z}^2$$

$$KE = \frac{1}{2}mA^2\omega^2 \sin^2(\omega t + \phi) \qquad \text{Eq. 36}$$

Using Eq. 12 and provided $\omega=\omega_0$

$$KE = \frac{1}{2}kA^2 \sin^2(\omega t + \phi) \qquad \text{Eq. 37}$$

The total energy of the system E_T is the sum of the potential and kinetic energy. Then, combining Eqs. 35 and 37

$$E_T = KE + U$$

$$E_T = \frac{1}{2}kA^2(\cos^2(\omega t + \phi) + \sin^2(\omega t + \phi))$$

$$E_T = \frac{1}{2}kA^2 \qquad \text{Eq. 38}$$

where A is the amplitude of oscillation and k is the spring constant. The average kinetic energy of the system can be computed by integrating Eq. 37

$$KE_{avg} = \frac{1}{T}\int_0^t \frac{1}{2}kA^2 \sin^2(\omega t + \phi)dt \qquad \text{Eq. 39}$$

The following are useful relationships to solve Eq. 39

$$\sin(A + B) = \sin A \cos B + \cos A \sin B$$

$$\sin(\omega t + \phi) = \sin\omega t \cos\phi + \cos\omega t \sin\ \phi$$

$$\sin^2(\omega t + \phi) = \sin^2(\omega t)\ \cos^2\phi + \sin\omega t \cos\omega t \sin\phi \cos\phi + \cos^2(\omega t) \sin^2\phi$$

$$+ \sin\omega t \cos\omega t \sin\phi \cos\phi$$

These integrals have solutions that follow from orthogonality. See for example the chapters on Fourier series by KA Stroud[34]. The average kinetic energy is equal to the sum of the integrals I_1 to I_4

$$kE_{avg} \equiv < KE > = \frac{1}{T}\frac{1}{2}KA^2(I_1 + I_2 + I_3 + I_4)$$

where,

$$I_1 = \cos^2\phi \int_0^{\top} \sin^2(\omega t)\, dt = \frac{T}{2}\cos^2\phi$$

$$I_2 = \sin^2\phi \int_0^{T} \cos^2(\omega t)\, dt = \frac{T}{2}\sin^2\phi$$

$$I_3 = I_4 = \frac{1}{2}\left[\int_0^{T} \sin\omega t \cos\omega t\, dt\right] \sin\phi \cos\phi$$

$$I_3 = I_4 = 0$$

$$< KE > = \frac{1}{T}\,\frac{1}{2}KA^2\frac{T}{2}[\sin^2\ \phi + \cos^2\ \phi]$$

$$\sin^2\phi + \cos^2\phi = 1$$

$$< KE > = \tfrac{1}{2}\left[\tfrac{1}{2}KA^2\right] = \tfrac{1}{2}E_T \qquad \text{Eq. 40}$$

Moreover, the average potential energy can be expressed as follows,

$$U_{avg} \equiv < U > = \tfrac{1}{2}kA^2\,\tfrac{1}{T}\textstyle\int_0^T \cos^2(\omega t + \phi)\, dt = \tfrac{1}{2}\,E_T \qquad \text{Eq. 41}$$

The above integrals are solved in a similar way to that described to get to Eq. 40. To understand the relationship between the average kinetic and potential energies, one can assume that the velocity is zero and see what happens to KE and U. For $\dot{z} = 0$

$$KE = \frac{1}{2}m(\dot{z})^2 = 0 \qquad \text{Eq. 42}$$

Eq. 42 implies that the total energy when $\dot{z} = 0$ is found as U. This will yield maximum potential energy at maximum displacement z=A when $\dot{z} = 0$

$$U|_{\substack{z=A \\ \dot{z}=0}} = \frac{1}{2}kz^2 = \frac{1}{2}kA^2 \qquad \text{Eq. 43}$$

Assuming the position is zero, the potential energy U is zero and all the energy is found a kinetic energy. Since KE is proportional to the velocity squared, the velocity is maximum at z=0

$$U|_{\substack{z=0 \\ \dot{z}=\max}} = \frac{1}{2}k(z)^2 = 0 \qquad \text{Eq. 44}$$

$$KE = \frac{1}{2}m\dot{z}^2 = \frac{1}{2}kA^2 \qquad \text{Eq. 45}$$

From Eq. 15, it follows that at z=0 the maximum velocity is found, and it can be written as

$$\dot{z}(\max) = \omega_0 A \qquad \text{Eq. 46}$$

This result is identical to what directly follows from de expression from instantaneous velocity

$$\dot{z} = -A\omega_0 sin\,(\omega t + \phi) \qquad \text{Eq. 48}$$

The above discussion is typical of the analyses on energy in simple harmonic motion. To exemplify the generality of this discussion, Fig. 8 shows the potential energy U function versus the separation of two hydrogen atoms. The assumption is that the force near equilibrium for the two atoms is approximately Hookean (Eq. 32). A similar example is discussed by both Tipler and Mosca and by Feynman when discussing oscillations. This is not coincidental,

rather, it shows that is it is useful to describe atomic phenomena in terms of simple atomic motion and in particular to interpret the phenomena in terms of energy.

The expression used to describe the force between atoms as shown in Fig. 8 can be found by differentiating the function U (Eq. 34) with distance x (or equivalently z). Then

$$F_x = -\frac{dU}{dx} = -k(x - x_1) \qquad \text{Eq. 49}$$

where x=x1 is defined as the neutral position for the two atoms, i.e., -kx=0. The implication is that the separation between the atoms will oscillate sinusoidally around x_1. In Fig. 8a the "true" potential energy for the atoms is shown as a function of separation x. For the case of hydrogen atoms discussed by Tipler and Mosca x_1= 0.74 nm. As shown in the scheme in Fig. 8b, the quadratic expression for U (Eq. 34) is only an approximation of the true potential energy between the atoms around x_1.

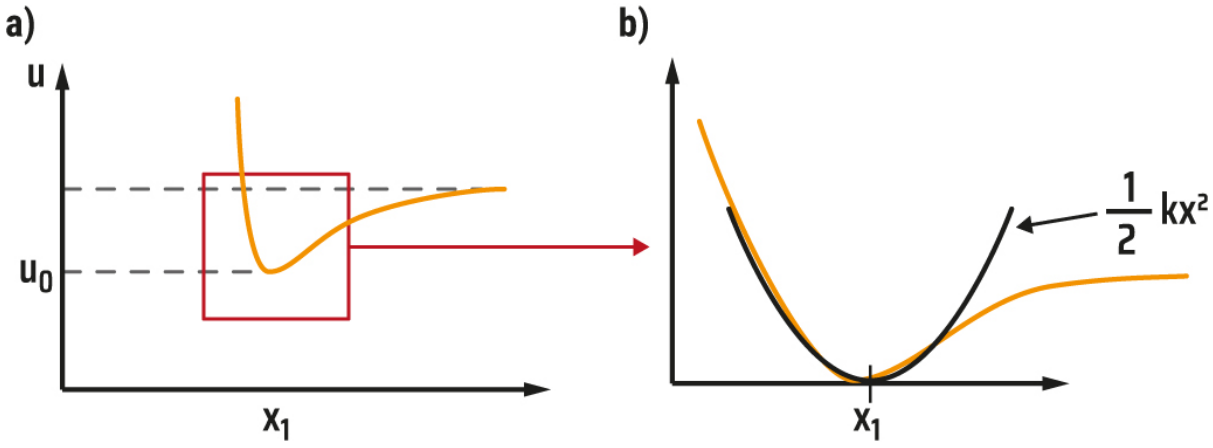

Figure 8. a) Schematic illustrating the relationship between the potential energy U between two hydrogen atoms and its equilibrium position. b) Schematic showing U as a function of x for a perfect Hookean potential, i.e., $1/2kx^2$, and the true potential between the two atoms. As observed the two potentials are similar when $x \approx x_1$.

1.6 Distance independent or constant forces

This section is dedicated to the addition of a constant force to the system. W recall that the investigation of Eq. 4 is the main focus of this text. This equation is written here again to discuss the terms already analysed on those to be analysed later.

$$m\ddot{z} + \frac{m\omega_0}{Q}\dot{z} + kz = F_0 \cos\ \omega t + F_{ts} \qquad \text{Eq. 50}$$

In summary, Eq. 50 is the full governing equation of motion of the cantilever that also allows us to understand the tip-sample force F_{ts} since the force is also represented. The main assumption so far is that the analysis is carried out for the first mode m=1.

So far the third term, i.e., kz, has been analysed in chapters 1.3 and 1.5. The dissipative term $m\omega_0/Q\dot{z}$ has been discussed in chapter 1.4. The terms on the right side of the equation have not been discussed yet. Only the drive force is discussed in the next chapters (chapters 1.8-1.10). The term F_{ts} is added in the second section. Before proceeding to those terms the following equation of motion will be considered

$$m\ddot{z} + kz\ + F_C = 0 \qquad \text{Eq. 51}$$

Tipler and Mosca discuss a similar example where the constant force F_C is represented by the gravitational force, i.e. F_C = mg. The force mg is distance independent in that both g and m are independent of position z. This is of course true for variations in z in the order of meters or less since it is well known that g depends on the distance with respect to the centre of the earth and these changes become significant when considering many km.

The model represented by the differential equation in Eq. 51 turns out to be meaningful in AFM since the tip-sample force in air might display a "plateau" in the proximity of the surface. Fig. 9 shows experimental force profiles[35]. F_{ts} as a function of tip-sample distance d but a plateau co be seen in one of the profiles. Here F_{ts} is normalised where minima are identified as -1. Minima in force in AFM are typically identified with the adhesion force F_{AD}. The force in black (Fig. 9) is a typical force profile where the force is negative, i.e., the tip and the sample attract

each other, for d > 0. For smaller values of d the force increases with decreasing distance. The force shown in black was obtained on a cleaved mica surface. On the other hand the force in orange displays a "plateau" of 2 nm where $F_{ts} \sim F_{AD}$. In this region the force is approximately constant. In 2013 we termed this region the SASS region[36] standing for small amplitude and small set point regime[35, 37-39].

The expected or standard force profile in air environments should be similar to that of the cleaved surface in Fig. 9 (black lines)[40] but in air environments we find that the plateau shown in orange lines might form with time[40-44]. It has been hypothesized that this plateau is a consequence of the aging of the surface whereby a nanometric layer of water and other contaminants forms on surfaces[26, 41, 43-44]. A schematic of this phenomenon is shown in Fig. 10a. A schematic of how the tip of an AFM would oscillate in the region of constant force is shown in Fig. 10b.

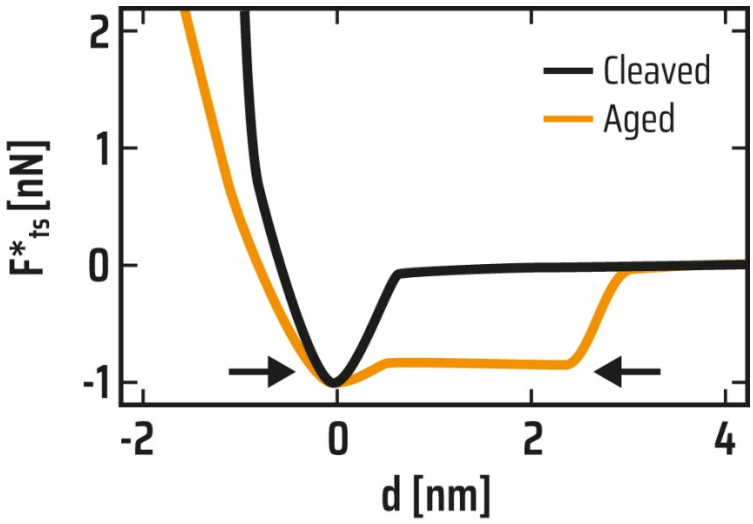

Figure 9. Force profiles where F_{ts} is plotted as a function of distance d. F_{ts} is normalized $F_{ts}^* = F_{ts}/F_{AD}$ by dividing by minima. The profile in black is for a tip interacting with a freshly cleaved mica surface and the orange one with an aged surface[35].

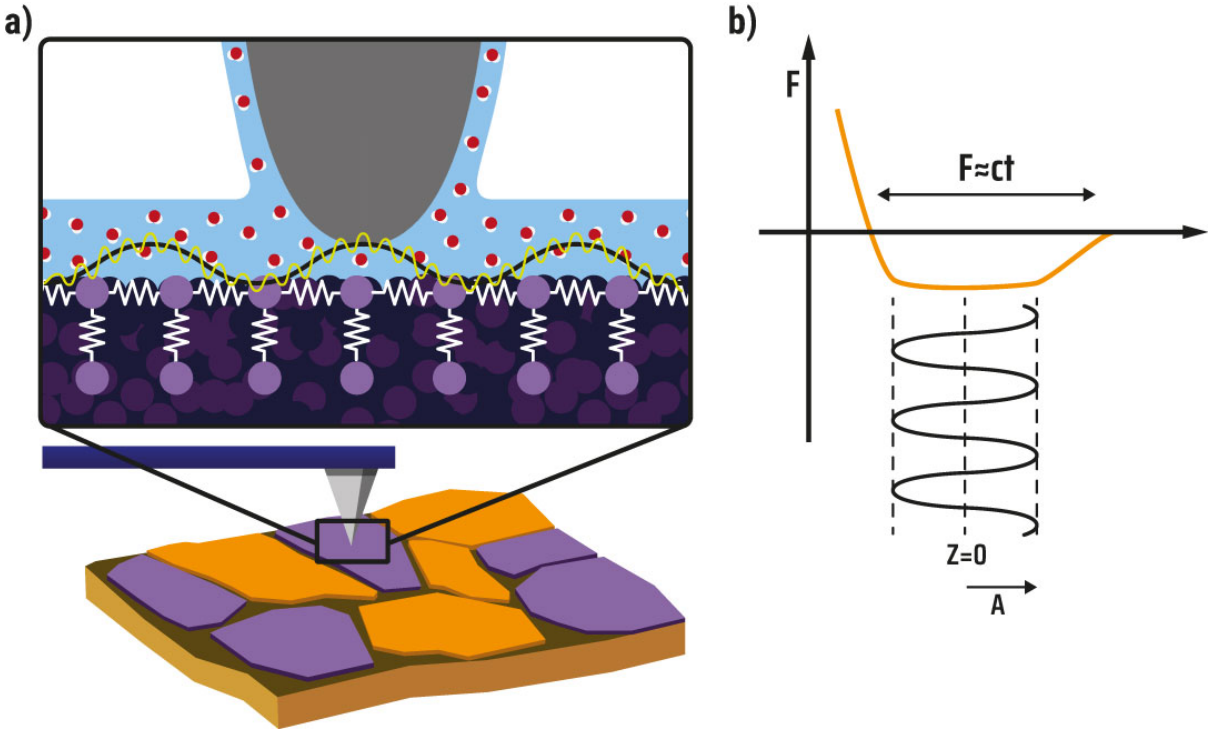

Figure 10. Illustration and schematic of a tip vibrating near a surface inside a hydration layer of water of height in the range of 1-2 nm. The force profile shows that the tip might oscillate within this layer where the force can be approximately constant.

The rheological model for the constant force is shown in Fig. 11. The following forces must be considered

$$m\frac{d^2z}{dt^2} = -kz + F_C \qquad \text{Eq. 52}$$

The value of F_C can be written in terms of k since in equilibrium and in the absence of oscillation

$$0 = -kz + F_C \qquad \text{Eq. 53}$$

$$kz = F_C \qquad \text{Eq. 54}$$

Eq. 54 allows us to write a new equilibrium position and coordinate axis z′,

$$z = \frac{F_C}{k} \equiv z_0 \; (z_0 => z' = 0) \qquad \text{Eq. 54}$$

The above expression (Eq. 54) can be used to determine the mean cantilever deflection z_0. This deflection is due to an average force $\langle F_{ts} \rangle$ equivalent to a constant force F_C in its effects on z_0. With the new equilibrium position at $z=z_0$ a new axis z' can be found from the diagram in Fig. 11. Then

$$m\frac{d^2(z'+z_0)}{dt^2} = -k(z'+z_0) + F_C = -kz' - kz_0 + F_C$$

$$m\frac{d^2z'}{dt^2} = -kz' \qquad \text{Eq. 55}$$

This expression is equivalent to Eq. 5 so the solution is also the same

$$z' = A\cos(\omega t + \phi) \qquad \text{Eq. 56}$$

The main result of adding a constant force is that if the tip oscillates in the region, or a region, of constant force, like the SASS region shown in Figs. 9 and 10, the behaviour is equivalent to simple harmonic motion. The only terms missing in this equation are the drive F_D, and dissipation.

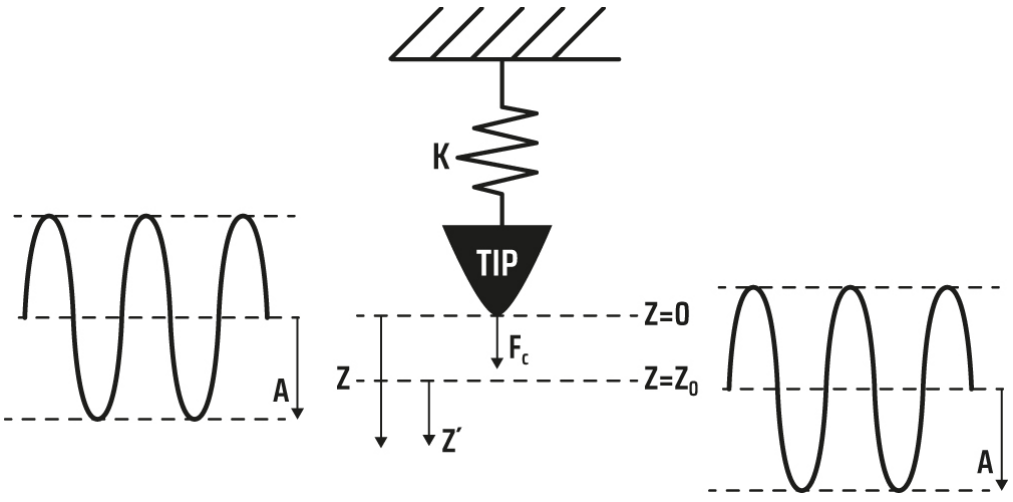

Figure 11. Schematic of the shift in reference from $z=0$ to $z'=0$ when $z=z_0$ due to the addition of a constant force F_C.

The potential energy in this case is

$$U = U_{\text{spring}} + U_{\text{constant force}} = \frac{1}{2}kz'^2 \qquad \text{Eq. 57}$$

The maximum potential energy is still

$$U = \frac{1}{2}kA^2 (U = 0 \text{ at } z' = 0 \; or \; z = \; z_0) \qquad \text{Eq. 58}$$

In SASS imaging, and assuming the ideal condition where F_{ts}=constant in the region, the force of adhesion can be found as[45]

$$F_{ts} \approx F_{AD} \approx kz_0 \qquad \text{Eq. 58}$$

In reality, since the amplitude of oscillation A might be larger than the range for which F_{ts}= constant (Fig. 10), the above expression is only a linear approximation. A more realistic interpretation of the phenomenon in SASS can be understood by considering the illustration in Fig. 12[39]. In the figure, an example is shown of the phenomenon where the cantilever interacts with the sample in the attractive mode only, i.e., $F_{ts} < 0$, with relatively large amplitudes A. Here, it is clear that the force is not constant. Another example is shown in the figure where the SASS mode of imaging occurs where $F_{ts} \approx F_{AD}$ and the oscillation amplitude is sufficiently small. As shown, it is possible that even if the force is not constant, for example, at the edges as also shown in Fig. 12 representing SASS imaging, the tip oscillates mostly and approximately at the bottom of the well. We see that the conditions are that[36, 46]

1) The range for which the $F_{ts} \approx$ constant must be approximately 2A, i.e., twice the amplitude of oscillation.

2) Second, the tip must be made to oscillate at the bottom of the well.

The first condition can be easily achieved since AFM allows the user to set any oscillation amplitude. The second condition is not trivial from an experimental point of view[46]. We have

recently shown that these conditions are still to be fully elucidated[38, 47]. It might be worth exploring these conditions in the future since they might lead to high resolution imaging[48-49] both because 1) of the small A conditions and because 2) the tip is in very close proximity to the sample where resolution is enhanced[50].

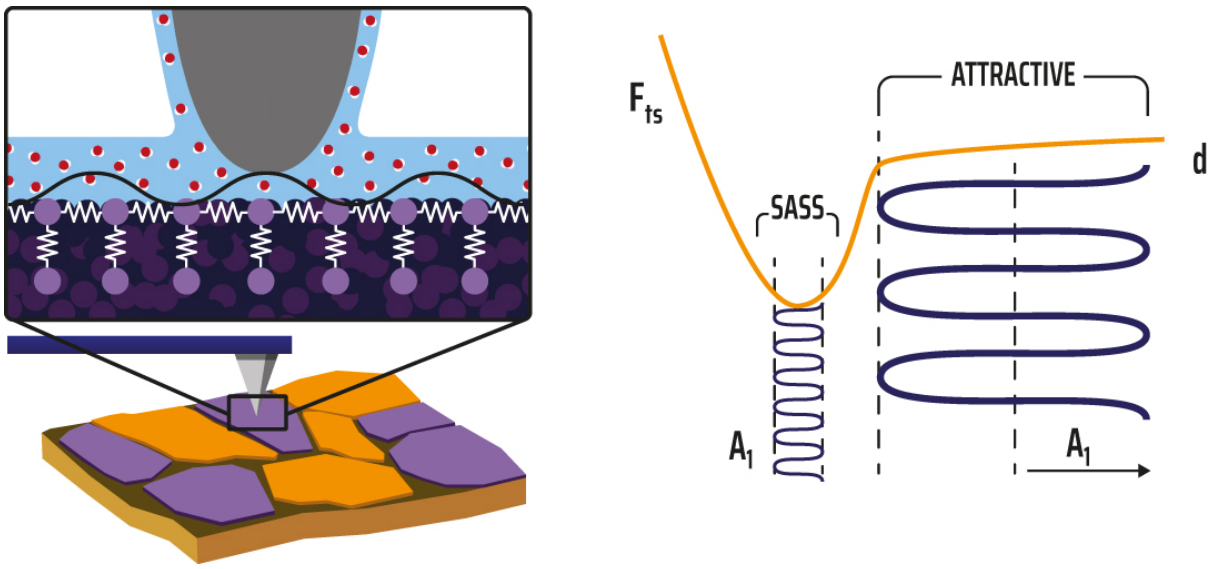

Figure 12. Schematic similar to that in Fig. 10 where an AFM tip oscillates inside a hydration layer and where relatively realistic force profiles are shown depicting how the tip can be made to oscillate in the attractive regime or within the well, i.e., in perpetual contact with the water layer.

1.7 Q factor and dissipation

The Q factor has been defined in chapter 1.4 and its relationship to dissipation has been already shown to some detail. Here, some physical interpretations will be discussed in terms of the derivations resulting from the equation of motion.

The equation of motion that accounts for dissipation (Eq. 17) is rewritten here

$$-kz - b\frac{dz}{dt} = m\frac{d^2z}{dt^2} \qquad \text{Eq. 59}$$

where all the terms have been already defined. The solution of this equation in terms of ω has been shown (Eq. 30) to be

$$\omega_r = \omega_0\sqrt{1 - \frac{1}{4Q^2}} \qquad \text{Eq. 60}$$

This is the resonant frequency in the presence of dissipation and no drive. Clearly, for any finite value of Q we have that $\omega_r < \omega_0$. We know that the solution is sinusoidal where $z \propto \cos(\omega t+\phi)$. In order to find the general solution Eqs. 23 and 24 were assumed to hold. The same assumptions are shown to aid the discussion

$$z = A_0 e^{i\omega t} \equiv z + iy \qquad \text{Eq. 61}$$

$$z = A_0 e^{i\omega t} \qquad \text{Eq. 62}$$

where the general solution can be written as before as

$$\omega = \frac{b}{2m}i \pm \omega_r \qquad \text{Eq. 63}$$

Inserting 63 into 62

$$z = A_0 e^{i(\frac{b}{2m}i+\omega_r)} = A_0 e^{-\frac{b}{2m}t} e^{\pm i\omega_r t} \quad \text{Eq. 64}$$

From Euler's identity the equation above can be written as

$$z = A_0 e^{-\frac{b}{2m}t}[\cos\ \omega_r t + i\sin\ \omega_r t] \quad \text{Eq. 65}$$

The real part of the solution can be written in a general form as

$$z = A_0 e^{-\frac{b}{2m}t} \cos\ (\omega_r t + \varphi) \quad \text{Eq. 66}$$

Importantly, Eq. 66 illustrates that the original amplitude A_0 decays with $-\frac{b}{2m}$. Therefore, this equation indicates that the energy of the oscillator is proportional to the square of the amplitude A_0 or simply proportional to A_0^2 and to the decaying expression $(e^{-\frac{b}{2m}t})^2$.

A typical definition follows from this derivation where τ is defined as

$$\frac{m}{b} = \tau \quad \text{Eq. 67}$$

Since the units of m are kg and those of b are kg/s, τ is expressed in units of time. In particular, the definition of τ is the time required for the oscillator's energy to diminish by a factor of 1/e. This can be shown as follows. From before (Eq. 38), the total stored energy in an oscillator is

$$E = \frac{1}{2}kA^2 \quad \text{Eq. 68}$$

Where, from Eq. 12, the following identity can be used to express k as

$$\mathrm{k} = m\omega_0^2 \qquad \text{Eq. 69}$$

Combining Eqs. 66 to 69

$$E = \frac{1}{2} m\omega_0^2 A_0^2 e^{-\frac{t}{\tau}} \qquad \text{Eq. 70}$$

When $t = 0$,

$$E_0 = \frac{1}{2} m\omega_0^2 A_0^2 \qquad \text{Eq. 71}$$

When $t = \tau$,

$$E_\tau = \frac{1}{2} m\omega_0^2 e^{-1} \qquad \text{Eq. 72}$$

and this concludes the proof. The final expression for the energy stored in an oscillator can be expressed as

$$E = E_0 e^{-\frac{t}{\tau}} \qquad \text{Eq. 70}$$

The above result (Eq. 70) assumes that there is dissipation and no drive (Eq. 5) meaning that the amplitude must decay with time. The expression can also be found in other ways, for example, by means of the energy dissipation expressed as

$$P_{dis} = \frac{dE}{dt} = F_{dis}\dot{z} = -b\dot{z}\dot{z} = -b\dot{z}^2 \qquad \text{Eq. 71}$$

It is clear that P_{dis} is the instantaneous dissipation and for this reason it can be written in terms of the derivative of the total energy with time.

Using Eq. 40,

$$< KE >\equiv \frac{1}{2}\left[\frac{1}{2}kA^2\right] = \frac{1}{2}E_T = \frac{1}{2}m < \dot{z} >^2$$

$$E_T = m < \dot{z} >^2 \qquad \text{Eq. 72}$$

Where the term in brackets is the average velocity. From the above expression the average velocity can be expressed in terms of E, m (or k and ω_0). Combining Eqs. 71 and 72 and assuming an average value for dE/dt (per cycle),

$$\frac{dE}{dt} = -b < \dot{z} >^2 = -b\frac{E}{m} \qquad \text{Eq. 73}$$

From this expression de differential of E can be expressed as a function of time,

$$\frac{dE}{E} = \frac{-b}{m}dt \qquad \text{Eq. 74}$$

Integrating and using $\Delta t = (t - t_0)$

$$\int_{E_0}^{E} \frac{dE}{E} = \frac{-b}{m}\Delta t$$

$$\ln\left(\frac{E}{E_0}\right)\Big|_{E_0=E/t_0} = \frac{-b}{m}\Delta t\Big|_{t_0=0}$$

$$E = E_0 e^{-\frac{b}{m}\Delta t} \qquad \text{Eq. 75}$$

Finally, using the definition $\tau=m/b$ from Eq. 67 and the fact that $t_0=0$,

$$E = E_0 e^{-\frac{t}{\tau}} \qquad \text{Eq.76}$$

This expression is equivalent to Eq. 70 and this competes the proof.

1.8 The driven oscillator

The topic of driven oscillations is closely related to resonance and all the concepts discussed so far are exploited in its analysis. The general equation is Eq. 5 rewritten here for completeness as Eq. 77

$$m\ddot{z} + \frac{m\omega_0}{Q}\dot{z} + kz = F_0 \cos\ \omega t + F_{ts} \qquad \text{Eq. 77}$$

The discussion in this chapter considers all the linear terms in the above expression, that is

$$m\ddot{z} + \frac{m\omega_0}{Q}\dot{z} + kz = F_0 \cos\ \omega t \qquad \text{Eq. 78}$$

The only term left out is F_{ts}, i.e., the nonlinear term. The object of the second section of the book is dedicated to the analysis of Eq. 77 including F_{ts}. Since much of the nonlinear analysis is based on the results of the linear analysis the results of this section are very important. The rheological model for Eq. 78 is shown in Fig. 13.

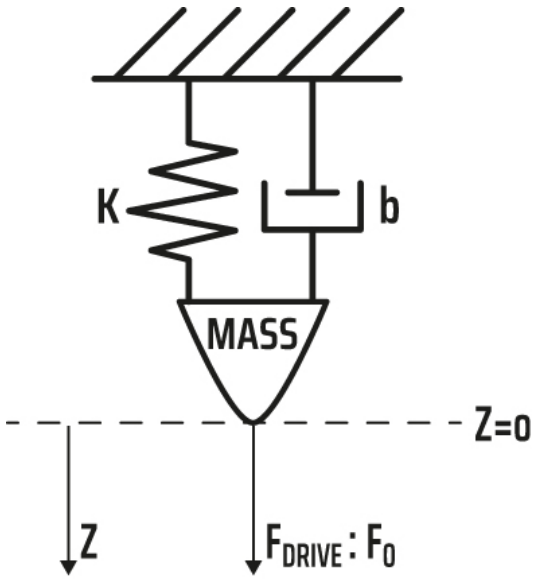

Figure 13. Rheological model corresponding to Eq. 78.

All the terms on the left hand side of Eq. 78 have been discussed already. We recall that the addition of dissipation, the second term in Eq. 78, shifts the resonant frequency from ω_0 to ω_r where $\omega_r < \omega_0$. This however does not imply that ω_0 is redefined as ω_r. Rather, we still have the phenomena occurring at $\omega = \omega_0$ and the phenomena occurring at $\omega = \omega_r$. In particular, in the presence of dissipation the maximum amplitude A occurs at $\omega = \omega_r$. However, we still have that $\phi = 90$ when $\omega = \omega_0$.

It is necessary to understand that Eq. 78 produces two solutions, a steady-state solution, and a transient solution. The transient solution is the same as that already analysed via the concepts in chapters 1.4 and 1.7 resulting in (Eq. 66),

$$z = A_0 e^{-\frac{t}{2\tau}} \cos\left(\omega_r' t + \varphi\right) \qquad \text{Eq. 79}$$

The transient solution is characterized by a resonant frequency that we term ω_r' in order to differentiate it from the resonant frequency that we will find in the presence of the driving force. Eq. 79 is also characterized by a phase shift φ that indicates that for an arbitrary time t, the phase is φ.

Nevertheless, The transient and the steady state solution "coexist" until the amplitude in Eq. 79 vanishes compared to the amplitude given by the steady state solution. Since the amplitude A in Eq. 79 is parametrized as a function of τ, the relevance of the transient solution, i.e., uncontrolled oscillation, depends on τ

$$z = A(t, \tau) \cos\left(\omega_r' t + \varphi\right) \qquad \text{Eq. 80}$$

From Eq. 67

$$\tau = \frac{m}{b} = \frac{Q}{\omega_0} \qquad \text{Eq. 81}$$

The implication is that for a given ω_0, the larger the Q the longer the transient solution persists. In amplitude modulation (AM) AFM, the amplitude must be constant. The implication is that the minimum time for scanning controllably, or the maximum scan rate, is limited by Q. As stated, the less dissipation the larger the Q. Thus, while working in vacuum environments and

low temperatures might be useful to minimize thermal noise, the value of Q is very high under such conditions. The implication is that, depending on the feedback, the scanning rate is further limited under vacuum. One must wait until the amplitude becomes approximately constant in order to operate the instrument in the amplitude modulation (AM) mode where the amplitude must remain constant. Otherwise noise will control the system and the image will be blurred. The opposite is true for liquid environments where Q is very low. Similar considerations can be drawn for frequency modulation (FM) where the frequency shift is to remain constant[50-51]. These concepts will be discussed in the second section of the book. Thus, the time required for these transitory solutions (Eq. 80) to vanish is crucial. Practically, this means that if the cantilever was driven really quickly, the oscillation amplitude would be dominated by the transient solutions, i.e., the dynamics of the cantilever would be controlled by the transient term $A_0 e^{-\frac{t}{2\tau}}$, making it impossible or difficult to maintain a constant amplitude. The purpose of the drive is to control and set a given amplitude as selected by the user. The solution controlled by the drive is that produced by the steady state. The object of this chapter is the steady state solution.

In the steady state, the oscillation amplitude should be kept constant. This is particularly true in AM AFM where A is used as feedback. The physical implication is that, in the steady state, all of the energy that the drive delivers to the system is dissipated by the viscous term at a constant rate. First the drive builds up the amplitude and later such equilibrium is reached. In the presence of transients, the system will continue to dissipate energy and decrease A until the amplitude is constant. When the cantilever is driven far from the surface this amplitude is typically termed A_0.

In AM AFM the phase shift ϕ will produce contrast (see chapters 2.1 to 2.11) while the amplitude should be (ideally) flat, i.e., there should be no error in A as the amplitude should remain constant. The contrast channel A is thus typically termed the error channel in AM AFM. However, in frequency modulation (FM), amplitude contrast is possible (see section 2) since what remains constant is the frequency shift and A can freely vary.

Since Eq. 78 consists of linear terms only, the method employed in chapter 1.4 (Eq. 17) to solve the equation is still valid. From there

$$z = Be^{i\omega t} \equiv x + iy \qquad \text{Eq. 82}$$

where if $z = x + iy$ is a solution of Eq. 17 so are x and y. Time derivatives produce the following result

$$z = Be^{i\omega t} \quad \text{Eq. 83}$$

$$\dot{z} = i\omega Be^{i\omega t} \quad \text{Eq. 84}$$

$$\ddot{z} = -\omega^2 Be^{i\omega t} \quad \text{Eq. 85}$$

Substituting Eqs. 83-85 into Eq. 78 gives

$$-m\omega^2 z + ib\omega z + m\omega_0^2 z = F_0 e^{i\omega t} \quad \text{Eq. 86}$$

From Eq. 83

$$e^{i\omega t} = \frac{z}{B} \quad \text{Eq. 87}$$

Then, the drive can be written in its complex form as

$$F_0 e^{i\omega t} \equiv \frac{F_0 z}{B} \quad \text{Eq. 88}$$

Combining Eqs. 86 and 88

$$\mathrm{B} = \frac{F_0}{m(\omega_0^2 - \omega^2) + ib\omega} \quad \text{Eq. 89}$$

Using the basics of complex numbers and Fig. 14

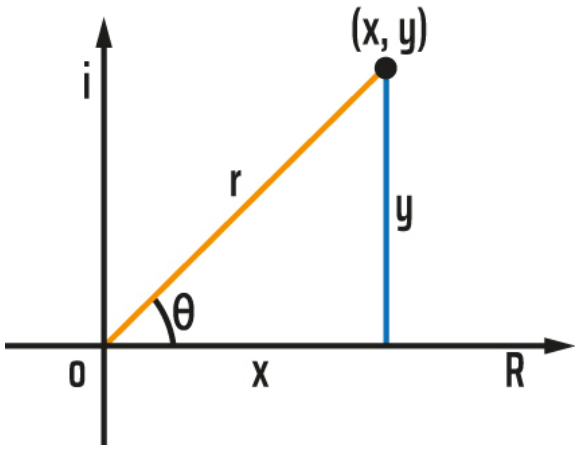

Figure 14. Schematic showing the relationship between a complex number written in its polar form and in its cartesian form.

From Fig. 14 the complex number z

$$z = x + iy \qquad \text{Eq. 90}$$

can also be expressed in polar form

$$z = re^{i\phi} = \sqrt{x^2 + y^2}e^{i\phi}$$

$$\tan\ \phi = \frac{y}{x} \qquad \text{Eq. 91}$$

The form in Eq. 91, and particularly the equation of the tangent of the phase ϕ, are very important in oscillation theory. Then, Eq. 89 can be written in polar form as

$$B = \frac{F_0}{z} = \frac{F_0}{x + iy}$$

where

$$z = m(\omega_0^2 - \omega^2) + ib\omega = \sqrt{m^2(\omega_0^2 - \omega^2) + b^2\omega^2}e^{i\phi}$$

and

$$\tan\phi = \frac{b\omega}{m(\omega_0^2 - \omega^2)} \qquad \text{Eq. 92}$$

Finally,

$$B = F_0 \frac{1}{\sqrt{m^2(\omega_0^2 - \omega^2) + b^2\omega^2}e^{i\phi}}$$

$$B = \frac{F_0 e^{-i\phi}}{\sqrt{m^2(\omega_0^2 - \omega^2) + b^2\omega^2}} \qquad \text{Eq. 93}$$

The above result implies that the complex solution of Eq. 17 (or equivalently Eq. 78) is,

$$z = Be^{i\omega t} = Ae^{i(\omega t - \phi)} \qquad \text{Eq. 94}$$

where both amplitude A and phase ϕ are determined from known parameters as follows

$$A = \frac{F_0}{\sqrt{m^2(\omega_0^2 - \omega^2)^2 + b^2\omega^2}} \qquad \text{Eq. 95}$$

and

$$\tan\ \phi = \frac{b\omega}{m(\omega_0^2 - \omega^2)} \qquad \text{Eq. 96}$$

It is important to notice the negative sign in Eq. 94. This negative sign can be written there or directly in Eq. 96. Feynman emphasizes that the negative sign should be in Eq. 96 since this directly indicates that z lags the drive. The full complex solution is

$$z = Be^{i\omega t} = Ae^{i(\omega t - \phi)}$$

$$z = A\cos(\omega t - \phi) + iAsin(\omega t - \phi) \qquad \text{Eq. 97}$$

It follows from linearity that both parts are solutions meaning that a solution to the driven oscillator is

$$z = A\cos(\omega t - \phi) \qquad \text{Eq. 98}$$

where the phase shift ϕ, i.e., the lag between the response and the driving force, is given by Eq. 96. In particular, the response always lags the force as shown in Fig. 15. In the figure the drive force has been written in terms of the drive amplitude A_D which is not equivalent to the drive force F_0. In terms of A_D the drive force is

$$F_D = kA_D \cos(\omega t) \qquad \text{Eq. 99}$$

where k is the cantilever's spring constant, and the position of the drive is identified with $z_D = A_D \cos(\omega t)$. The rheological model discussing the drive force in terms of Eq. 99 is discussed in chapter 1.10. In particular Eq. 99 s equivalent to

$$F_D = F_0 \cos(\omega t) \qquad \text{Eq. 100}$$

The implication is that $F_0 = kA_D$. Anczykowski et al. [23] elaborated a theory, i.e., rheological model and expressions (see chapter 1.10), where the interested reader can learn more about this approach. By comparing Eqs. 99 or 100 to Eq. 98, the lagging of z with respect to the drive force can be plotted as a graph (Fig. 15).

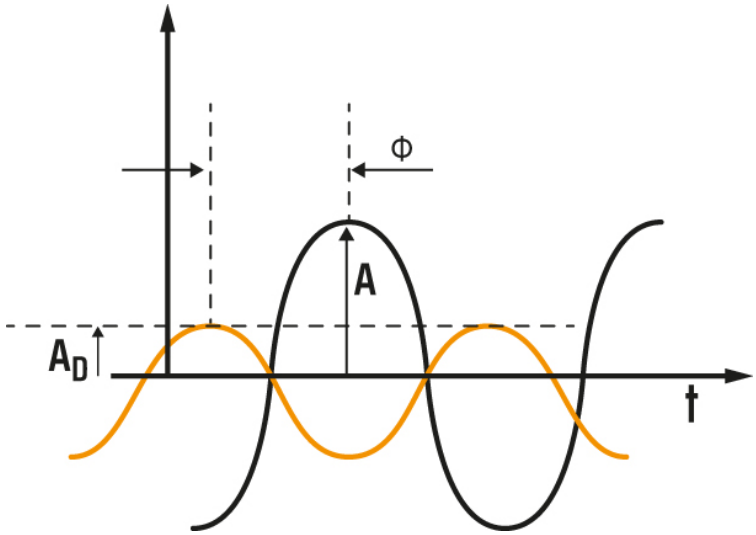

Figure 15. Illustration of the lagging of $z = A\cos(\omega t - \phi)$ with respect to $F_D = kA_D\cos(\omega t)$.

Summary of chapter 1.8.

As a main result, it is worth noting that all parameters in A (Eq. 95) and in ϕ (Eq. 96) can be experimentally found when calibrating the cantilever in AFM. For example, Fig. 16 shows a standard frequency sweep acquired with a cypher AFM (Oxford Instruments) at a large enough distance from the surface so that $F_{ts} \rightarrow 0$. Under such conditions the linear equation Eq. 78 applies. It can be shown that[31] Q, ω_0, ω_r and k can be derived from such sweeps. This means that expressions can be found to relate frequency sweeps, or other experimental data or identities, to these parameters. Such expressions are exploited in AFM software. Some of the relationships have been developed so far in the chapters above.

For example, we have already shown how ω_r is obtained when there is dissipation, i.e., ω_r is that frequency which gives a maximum A in a frequency sweeps such as that in Fig. 16. In the next chapter we show how to relate ω_r to ω_0, so ω_0 can be indirectly computed from ω_r and Q (experimentally finding ω_r is easy since it is the ω of maximum amplitude in a sweep like that in Fig. 16) Note that another expression for ω_r was already found in chapter 1.4 when dissipation was allowed. The presence of a driving force however leads to another expression for ω_r. In the next chapter we also show how to compute Q directly from a frequency sweep such as that in Fig. 16. The spring constant k can be measured I many ways in AFM{Sader, 2012 #99}. For example, looking at a force versus displacement curve. Otherwise the cantilever manufacturer typically provides data on k.

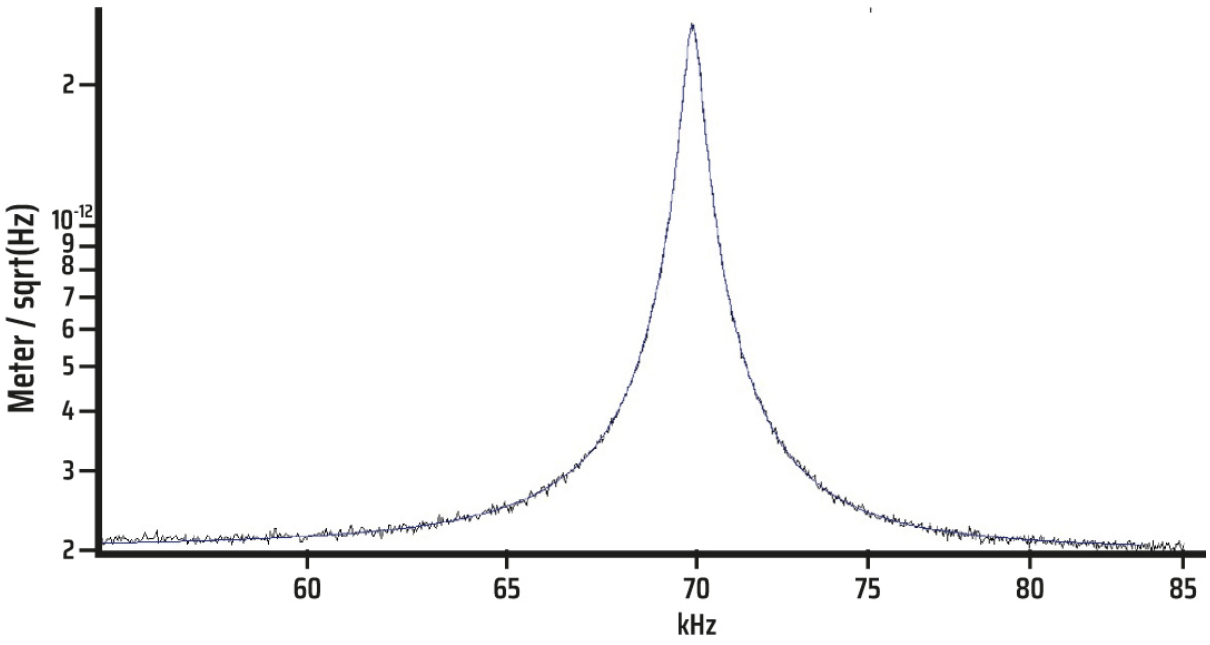

Figure 16. Standard frequency sweep in AFM where the resonance curve is seen to peak at $f_r \approx 70$ kHz. The finite width of the curve indicates that there is dissipation. Thus Q takes on a finite value. Here the value of Q was approximately 100. The implication is that $\omega_r < \omega_0$. The phase shift is 90 at ω_0 while the amplitude A is maximum at ω_r.

1.9 The driven oscillator and resonance with a driving force

This section elaborates on the relationships between the Q factor, dissipation, ω_0, ω_r and driven response.

First, Eq. 95 provides the means to find the maximum value of A as a function of drive frequency ω. In AFM the drive frequency can be arbitrarily selected by the user. In particular, in AFM both F_0 and ω can be arbitrarily selected. This determines the drive force as observed from Eq. 100, i.e., $F_D = F_0 \cos(\omega t)$.

The amplitude is (Eq. 95),

$$A = \frac{F_0}{\sqrt{m^2(\omega_0^2 - \omega^2)^2 + b^2\omega^2}} \qquad \text{Eq.101}$$

Equation the derivative with ω to zero gives the maximum amplitude A_{max}

$$\frac{dA}{d\omega} = 0 \Rightarrow A_{max}$$

$$\omega_r|_{A=A_{\max}} = \omega_0 \left[1 - \frac{1}{2Q^2}\right]^{1/2} \qquad \text{Eq.102}$$

The value Amax determines ω_r. Again $\omega_r < \omega_0$. This resonance is different from that found in the presence of dissipation and the absence of drive (compare with Eq. 30). This result can be obtained algebraically, but it is easier to confirm it by exploiting computing software such as Matlab. The script below provides the result in Eq. 102. In the script w_ratio=ω/ω_0 has been introduced to simplify Eq. 101.

Matlab script to solve Eq. 101 and produce Eq. 102.

```
clear all
clc

syms Q w_ratio

y1= ((1-(w_ratio)^2)^2+(w_ratio/Q)^2)^0.5;

diff_w = diff(y1, w_ratio )

solve_w = solve(diff_w ==0, w_ratio)
```

Fig. 17 shows a relevant part of a frequency sweep obtained by plotting Eq. 101. In the vertical axis A is plotted and in the horizontal axis ω is plotted normalized in terms of ω_0, i.e., ω/ω_0. Only the region for $0.9 < \omega/\omega_0 < 1.1$ is shown in order to showcase that the maximum amplitude A does not result at $\omega/\omega_0=1$. This is in agreement with Eq. 102. The phase shift ϕ however is still 90° where $\omega=\omega_0$. This can be confirmed from Eq. 96. The curve is that of the linear response from Eq. 78.

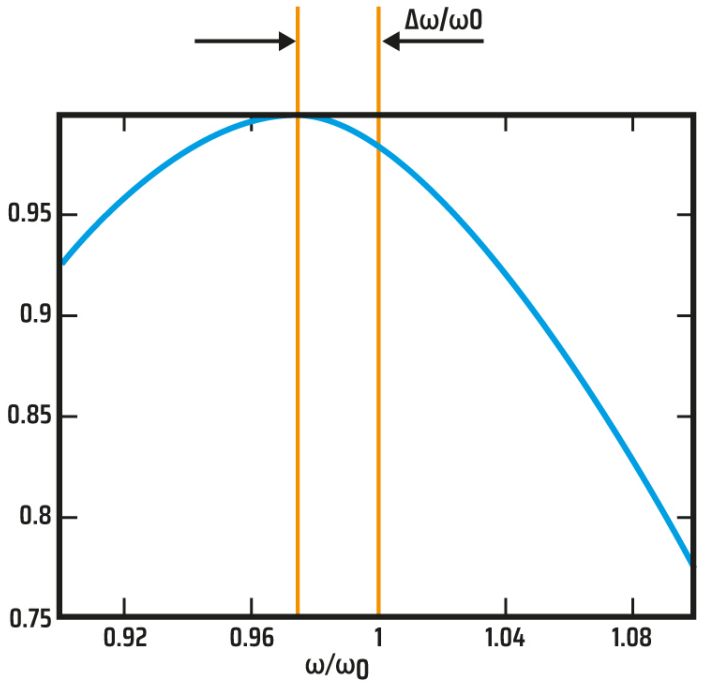

Figure 17. Part of a frequency sweep obtained by plotting Eq. 101 where A is plotted against the normalized frequency ω/ω_0. The maximum value of A, i.e., A_{max}, does not coincide with ω_0. Rather A_{max} occurs when $\omega_r/\omega_0 < 0$. The actual value of ω_r is found from Eq. 102.

There is a way to derive an expression for the Q factor in terms of a frequency sweep as shown in Fig. 17. A schematic showing relevant parameters for such derivation is shown in Fig.18. The first thing to note is that for the derivation to hold $\omega_r \approx \omega_0$. This happens when Q is large enough. The larger Q the better the following derivation holds. The amplitude A in Fig. 18 is parametrized by ω, i.e., the drive frequency. Then, from Eq. 101 and since the power of the system is proportional to the square of the amplitude (Eq. 38)

$$A^2 = \frac{F_0^2}{m^2(\omega_0^2 - \omega^2)^2 + b^2\omega^2} \qquad \text{Eq.103}$$

In his lectures on resonance, Feynman works also with the square of the amplitude since the derivation of Q follows from the A^2 versus ω curve. Feynman further proposed to the readers to find the relationship between Δω as shown in Fig. 18. This solution must be found in terms of the square of the amplitude, i.e., the term proportional to power or stored energy.

Here, such relationship is derived as follows. If we term the maximum amplitude squared A_0^2, the objective is to find $A^2 = \frac{1}{2}A_0^2$ analytically. This will relate Δω to ω_0 and Q. It follows that some assumptions make this relatively easy. First, following the advice of Feynman in his lectures, we assume that $\omega_r \cong \omega_0$ (this assumption is key since the relationship to be found will hold only for large values of Q). It follows that

$$\omega_0^2 - \omega^2 \approx (\omega_0 - \omega)2\omega_0 \qquad \text{Eq.104}$$

Then,

$$A^2 = \frac{F_0^2}{m^2\left(\omega_0^2 - \omega^2\right)^2 + b^2\omega^2} \approx \frac{F_0^2}{4\omega_0^2 m^2(\omega_0 - \omega)^2 + b^2\omega^2} \qquad \text{Eq. 105}$$

The following identity can also be employed to simplify the equation and write Eq. 105 in term of Q

$$b^2\omega^2 = \frac{m^2\omega_0^2\omega^2}{Q^2} \qquad \text{Eq. 106}$$

We also recall that, by definition,

$$\gamma = \frac{\omega_0}{Q} \qquad \text{Eq. 107}$$

Combining Eqs. 105 and 106 the general expression for the amplitude as a function of ω is

$$A^2 \approx \frac{F_0^2}{4\omega_0^2 m^2\left[(\omega_0-\omega)^2+\left[\frac{\omega}{2Q}\right]^2\right]}$$

$$A^2 \approx \frac{F_0^2}{4\omega_0^2 m^2\left[(\omega_0-\omega)^2+\left[\frac{\gamma}{2}\right]^2\right]} \qquad \text{Eq. 108}$$

In Eq. 108 it has been assumed that when $\omega \approx \omega_0$, the width of the curve in Fig. 18 is $\omega = \omega_0 + \Delta\omega/2$ where $\gamma = \frac{\omega_0}{Q} \approx \frac{\omega}{Q}$. This last assumption is key and holds only for large Q.

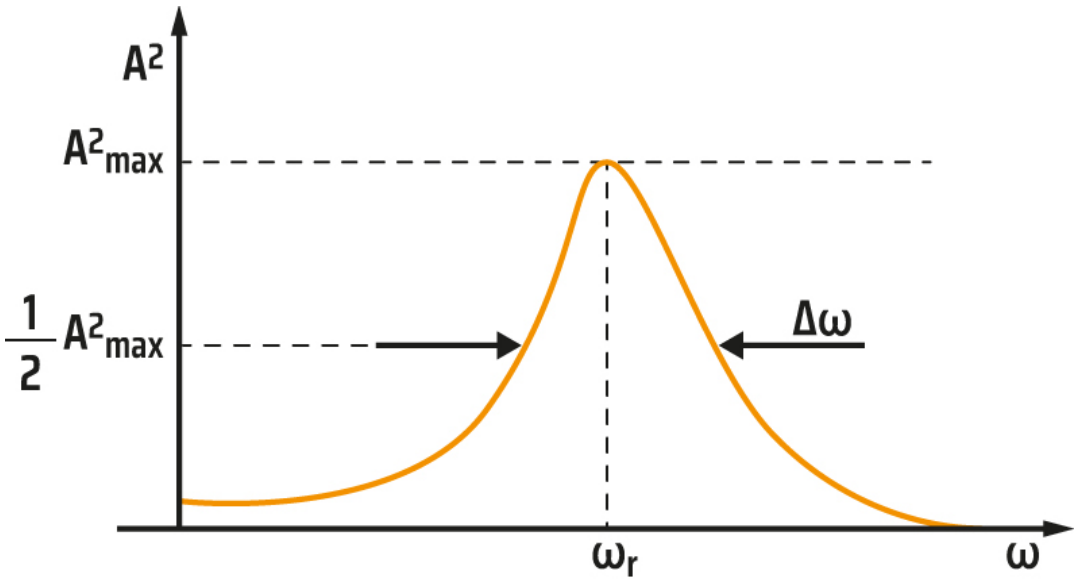

Figure 18. Amplitude squared A2 versus frequency ω where the width Δω at half power is shown.

With the above assumption Eq. 108 can be further simplified

$$A^2 \approx \frac{F_0^2}{4k^2\left[\left(1-\frac{\omega}{\omega_0}\right)^2+\left[\frac{1}{2Q}\right]^2\right]} \qquad \text{Eq. 109}$$

The maximum stored energy occurs at maximum amplitude A_0, or stored energy, which is proportional to the square of the amplitude. This has been shown to result (Eq. 102) when $\omega = \omega_r$ where $\omega_r \approx \omega_0$ if Q is large enough. Then

$$A_0^2 \approx \frac{F_0^2}{4k^2\left[\frac{1}{2Q}\right]^2}$$

$$A_0^2 \approx \left[\frac{F_0 Q}{k}\right]^2 \qquad \text{Eq. 110}$$

The above (Eq. 110) is a typical result employed in AFM to compute the drive force F_0 in Newtons in terms of the observables A_0, k and Q when working at or near resonance. The square of the amplitude at half maximum occurs when $\Delta\omega = 2|(\omega_0 - \omega)|$ as illustrated in Fig. 18. The square of the amplitude at $1/2A_0^2$ ($\Delta\omega$) can be found from Eq. 109

$$A^2(\omega = \omega_0 \pm \Delta\omega) \approx \frac{F_0^2}{4k^2\left[\left(1-\frac{\omega}{\omega_0}\right)^2+\left[\frac{1}{2Q}\right]^2\right]}$$

$$A^2(\omega = \omega_0 \pm \Delta\omega) \approx \frac{F_0^2}{4k^2\left[\left(1-\frac{\omega_0 \pm \Delta\omega/2}{\omega_0}\right)^2+\left[\frac{1}{2Q}\right]^2\right]}$$

$$A^2(\omega = \omega_0 \pm \Delta\omega) \approx \frac{F_0^2}{4k^2\left[\left(\frac{\pm\Delta\omega}{2\omega_0}\right)^2+\left[\frac{1}{2Q}\right]^2\right]} \qquad \text{Eq. 111}$$

Since the drive frequency at maximum amplitude can be written as $\omega = \omega_0 \pm \Delta\omega/2$. Combining the constraint $A^2 = \frac{1}{2}A_0^2$ and Eqs. 110 and 111

$$\frac{1}{2}\left[\frac{F_0 Q}{k}\right]^2 = \frac{F_0^2}{4k^2\left[\left(\frac{\pm\Delta\omega}{2\omega_0}\right)^2 + \left[\frac{1}{2Q}\right]^2\right]}$$

$$2Q^2 = \frac{1}{\left[\left(\frac{\pm\Delta\omega}{2\omega_0}\right)^2 + \left[\frac{1}{2Q}\right]^2\right]}$$

$$\left(\frac{\pm\Delta\omega}{2\omega_0}\right)^2 2Q^2 + \frac{2Q^2}{[2Q]^2} = 1$$

$$\left(\frac{\pm\Delta\omega}{2\omega_0}\right)^2 2Q^2 + \frac{1}{2} = 1$$

$$\left(\frac{\pm\Delta\omega}{2\omega_0}\right)^2 = \frac{1}{[2Q]^2} \qquad \text{Eq. 112}$$

Eq, 112 shows that the Q factor is related to the width of the resonance curve Δω (Fig. 18) as follows

$$\frac{\Delta\omega}{\omega_0} = \frac{1}{Q} \qquad \text{Eq. 113}$$

It is interesting to see how other interesting relationships follow from Eq. 113

$$\frac{\Delta\omega}{\omega_0} \approx \frac{1}{Q} \approx \frac{\Delta f}{f_0}$$

$$\Delta\omega = \frac{\omega_0}{Q} \equiv \gamma$$

$$\Delta\omega Q = \omega_0 \qquad \text{Eq. 114}$$

1.10 Other derivations of Q and energy considerations in the linear model

The work done by the drive in the steady state must be equal to the energy dissipated via the viscous term contained in the equation describing the driven oscillator (Eq. 78)

$$F_D = F_0 \cos\ \omega t \qquad \text{Eq.115}$$

$$m\ddot{z} + \frac{m\omega_0}{Q}\dot{z} + kz = F_0 \cos\ \omega t \qquad \text{Eq.116}$$

The work done by the drive is expressed in its differential form as

$$dz = \dot{z}dt$$

$$dW = F_D dz \qquad \text{Eq. 117}$$

Where, from Eq. 98

$$\dot{z} = -\omega A \sin\,(\omega t - \phi) \qquad \text{Eq.118}$$

Finally, the work done per cycle results from combining Eqs. 116 to 118

$$W_D = \int_0^T F_D \cdot \dot{z}dt$$

$$W_D = -F_0 A\omega \int_0^T \sin\,(\omega t - \phi)\cos\omega t dt$$

$$W_D = -F_0 A\omega \int_0^T (\sin(\omega t)\cos\phi - \cos(\omega t)\sin\phi)\cos\omega t dt$$

$$W_D = F_0 A\omega \left[\int_0^T \cos^2(\omega t)dt\right] \cdot \sin\ \phi \qquad \text{Eq.119}$$

Th above results from the orthogonality between the cosine and the sine functions. Solving E. 119, the work done per cycle by the drive is

$$W_D = F_0 A\omega \left[\frac{T}{2}\right] \sin\ \phi$$

$$T = \frac{2\pi}{\omega}$$

$$W_D = \pi F_0 A sin\phi \qquad \text{Eq.120}$$

The physical interpretation of Eq. 120 is that the maximum work done per cycle by the drive occurs approximately when sinϕ=1, namely, when , from Eq. 96, ω = ω_0. This definition is approximate only because WD multiplies A and sinϕ and A is not maximum when sinϕ=1. The implication is that sinϕ=1 does not coincide with the value ω=ω_r that produces the maximum amplitude either. The implication is that the phase shift is approximately 90° for the maximum work done by the drive. Importantly, it will be shown in section 2 (Eq. 2.35) that the same expression is found when computing the energy dissipated by the nonlinear term F_{ts}.

The differential of the energy dissipated dE by the viscous term in Eq. 116 is given by the differential equation

$$dz = \dot{z}dt$$

$$\mathrm{dE} = F_b \cdot dz \qquad \text{Eq. 121}$$

Then, the energy dissipate per cycle by the viscous force follows by solving the following integral

$$\mathrm{E} = \int_0^T F_b \cdot \dot{z}dt$$

$$\mathrm{E} = \int_0^T \frac{m\omega_0}{Q}\dot{z}\cdot\dot{z}dt$$

$$\mathrm{E} = \frac{m\omega_0}{Q}\int_0^T [\omega \mathrm{A}\sin(\omega t - \phi)]^2 dt$$

$$E = \frac{m\omega_0}{Q}\omega^2 A^2 \int_0^T [\sin(\omega t)\cos\phi - \cos(\omega t)\sin\phi]^2 dt$$

$$E = \frac{m\omega_0}{Q}\omega^2 A^2 \int_0^T \{[\sin(\omega t)\cos\phi]^2 + [\cos(\omega t)\sin\phi]^2 - 2\sin(\omega t)\cos(\omega t)\sin\phi\cos\phi\} dt$$

$$E = -\frac{m\omega_0}{Q}\omega^2 A^2 \int_0^T \{[\sin(\omega t)\cos\phi]^2 + [\cos(\omega t)\sin\phi]^2\} dt$$

$$E = -\frac{m\omega_0}{Q}\omega^2 A^2 \int_0^T \{[\sin(\omega t)]^2 cos^2\phi + [\cos(\omega t)]^2 sin^2\phi\} dt$$

$$E = -\frac{m\omega_0}{Q}\omega^2 A^2 \left\{\frac{T}{2}cos^2\phi + \frac{T}{2}sin^2\phi\right\}$$

$$E = -\frac{m\omega_0}{Q}\omega^2 A^2 \frac{T}{2}[cos^2\phi + sin^2\phi]$$

$$E = -\frac{m\omega_0}{Q}\omega A^2\pi \qquad \text{Eq. 122}$$

The Q factor can now be expressed as a function of energy dissipation per cycle normalized by the total energy. Eq. 122 is also equivalent to that found when developing the nonlinear theory (Eq. 2.37). The total stored energy is E_T (Eq. 38)

$$E_T = \frac{1}{2}kA^2 \qquad \text{Eq.123}$$

The ratio between Eq. 122 and Eq. 123 is, by assuming $\omega \approx \omega_0$,

$$\frac{|[E]_{cycle}|}{E_T} = \frac{\frac{k}{Q}A^2\pi}{\frac{1}{2}kA^2}$$

$$\frac{|[E]_{cycle}|}{E_T} = \frac{2\pi}{Q} \qquad \text{Eq. 124}$$

It follows that the energy dissipated per cycle by the viscous term, or equivalently (see Eq. 126 and discussion), the work done by the drive per cycle, is 2π divided by Q. As expected, the larger the Q the smaller this ratio. The implication is that the larger the Q factor the longer it takes for the system to lose energy via the viscous term.

Finally, the average power dissipated per cycle is simply Eq. 122 divided by T

$$< P >= \frac{E}{T} = \frac{1}{2}\frac{m\omega_0}{Q}\omega^2 A^2 \qquad \text{Eq. 125}$$

If, as in the case of the driven oscillator in the steady state, all the power of the drive is dissipated by the dissipative term, Eq. 125 should be the same as Eq. 116. This can be shown as follows

$$< \mathrm{P} >= \frac{W_D}{T} = \frac{\pi F_0 A sin\phi}{T}$$

$$< \mathrm{P} >= \frac{1}{2}F_0\omega A sin\phi \qquad \text{Eq. 126}$$

Looking at the energy delivered by the drive instead (Eq. 120), and if in the steady state all the energy dissipated per cycle must be delivered by the drive, it follows that

$$W_D = \pi F_0 A sin\phi$$

$$\frac{|[W_D]_{cycle}|}{E_T} = \frac{\pi F_0 A sin\phi}{\frac{1}{2}kA^2} \qquad \text{Eq. 127}$$

If $\omega \approx \omega_0$, it follows from the general expression for A as a function of ω for the driven oscillator (Eq. 95) that

$$F_0 = \frac{kA}{Q} \qquad \text{Eq. 128}$$

Combining Eqs. 127 and 128

$$\frac{[W_D]_{cycle}}{E_T} = \frac{\pi \frac{kA}{Q} A sin\phi}{\frac{1}{2}kA^2}$$

$$\frac{[W_D]_{cycle}}{E_T} = \frac{2\pi}{\mathrm{Q}} sin\phi \qquad \text{Eq. 129}$$

Since $\omega \approx \omega_0$, $\sin\phi=1$. This follows from Eq. 96. Then

$$\frac{[W_D]_{cycle}}{E_T} = \frac{2\pi}{\mathrm{Q}} \qquad \text{Eq. 130}$$

As expected, Eq. 130 is equivalent to Eq. 124 when $\sin\phi=1(\omega\approx\omega_0)$

From Eq. 114 a relationship with $\Delta\omega$, or the width of the curve (Fig. 18), can be found

$$\frac{[W_D]_{cycle}}{E_T} = 2\pi \frac{\Delta\omega}{\omega_0} \qquad \text{Eq. 131}$$

If follows that the energy dissipated per cycle can be easily found from the geometry of the frequency seep (see Fig. 18). This result is very useful since it allows to determine the Q factor, the power of the drive and the energy dissipated by the vicus term by inspection of a frequency sweep.

Another way of looking at the drive

As stated, some authors[23] express the drive as kz_D. See Eq. 99. Then the position of the drive is

$$z_D = A_D \cos(\omega t) \qquad \text{Eq. 132}$$

The drive force is derived from the rheological model in Fig. 19

$$F_D = k[z(t) - z_D(t)] \qquad \text{Eq. 133}$$

where, as usual, the position of the point-mass is

$$z(t) = Acos(\omega t - \phi) \qquad \text{Eq. 134}$$

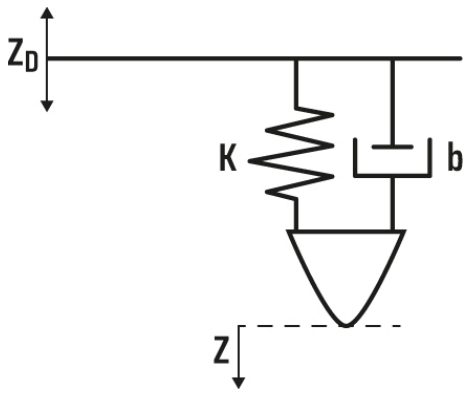

Figure 19. Rheological model describing the drive force in terms of k and the position of the drive z_D relative to the mass.

The power delivered by the drive per cycle can now be written as follows

$$< P_D >= \frac{1}{T}\int_0^T F_D \dot{z}_D \, \mathrm{d}t \qquad \text{Eq. 135}$$

Combining Eqs. 132-135

$$< P_D >= -\frac{1}{T}\int_0^T k[z(t) - z_D(t)]\dot{z}_D \, \mathrm{d}t$$

$$< P_D >= -\frac{1}{T}\int_0^T k[Acos(\omega t - \phi) - A_D \cos(\omega t)\,] - A_D \omega \sin(\omega t) \, \mathrm{d}t$$

$$< P_D >= -\frac{k}{T}\int_0^T -AA_D \omega cos(\omega t - \phi)\sin(\omega t) + \omega A_D^2 \cos(\omega t)\sin(\omega t) \, \mathrm{d}t$$

$$< P_D >= \frac{k}{T}\int_0^T AA_D \omega cos(\omega t - \phi)\sin(\omega t) \, \mathrm{d}t \qquad \text{Eq. 136}$$

where, from orthogonality, we obtained the result in Eq. 136. Solving the integral

$$< P_D >= \frac{AA_D k\omega}{T}\sin(\phi)\int_0^T sin^2(\omega t) \, \mathrm{d}t$$

$$< P_D >= \frac{AA_D k\omega}{T}\frac{T}{2}\sin(\phi)$$

$$< P_D >= \frac{1}{2} AA_D k\omega \sin(\phi) \qquad \text{Eq. 137}$$

The power delivered (Eq. 126) by the drive when modelling the drive as shown in Eq. 115 should be the same as that obtained in Eq. 137. In short

$$F_D = F_0 \cos\ \omega t \qquad \text{Eq. 138}$$

$$< P_D > = \frac{1}{2} F_0 \omega A sin\phi \qquad \text{Eq. 139}$$

Combining Eqs. 137 and 139

$$\frac{1}{2}\ AA_D k\omega \sin(\phi) = \frac{1}{2} AF_0 \omega sin\phi$$

$$F_0 = kA_D \qquad \text{Eq. 140}$$

This concludes the proof. The above expression, Eq. 140, can be employed to relate the drive amplitude A_D to the drive force F_0. Combining Eqs. 140 and 95

$$A = \frac{F_0}{\sqrt{m^2(\omega_0^2 - \omega^2)^2 + b^2\omega^2}}$$

$$F_0 = kA_D$$

$$F_0 = A\sqrt{m^2(\omega_0^2 - \omega^2)^2 + b^2\omega^2}$$

$$\sqrt{m^2(\omega_0^2 - \omega^2)^2 + b^2\omega^2} = kA_D \qquad \text{Eq. 141}$$

The above expression can be simplified by using $k = m\omega_0^2$

$$kA_D = Am\sqrt{(\omega_0^2 - \omega^2)^2 + \frac{\omega_0^2\omega^2}{Q^2}}$$

$$kA_D = kA\sqrt{\left(1 - \frac{\omega^2}{\omega_0^2}\right)^2 + \frac{\omega^2}{\omega_0^2 Q^2}}$$

$$A_D = A\sqrt{\left(1-\frac{\omega^2}{\omega_0^2}\right)^2+\frac{\omega^2}{\omega_0^2 Q^2}} \qquad \text{Eq. 142}$$

The expression in Eq. 142 is important in that it relates A_D with A in terms that can be found by inspecting a frequency sweep. In short, since Q, A and ω_0 can be experimentally, and easily, found, A_D can be easily determined indirectly. The main body of this books has been, so far, to determine these parameters, i.e., Q, ω_r, etc., from experimental observables. The drive frequency ω is easily set and known in AFM.

Finally at $\omega=\omega_0$

$$A_D = A\sqrt{\frac{1}{Q^2}}$$

$$A_D = \frac{A}{Q} \qquad \text{Eq. 143}$$

As a final note, in dynamic AFM, where the cantilever is driven analogously to the driven oscillator discussed here, and when the cantilever is driven far from the surface, the linear equation (Eq. 78) approximately applies. Then if we term the amplitude far from the surface the free amplitude A_0, i.e., the amplitude of oscillation in the absence of tip-sample force, the expression for A_D directly follows from observables

$$A_D = \frac{A_0}{Q} \qquad \text{Eq. 144}$$

The above expression is typically used in dynamic AFM, and, as noted, this expression is derived from the linear theory analysis in section 1 (chapters 1.1 to 1.10) of this book.

1.11 Summary

The linear theory discussed in this section is very important both to the AFM field and to many other much broader fields. For this reason, whatever can be learnt from the liner theory can be easily applied across fields. Furthermore, there is always something new to learn about oscillation theory. As an example, the reader can check a 2022 paper where oscillators are employed to model complex phenomena such as brain activity in the field of functional Magnetic Resonance Imaging (fMRI). In short, the concepts employed in fMRI are the same as those discussed through chapters 1.1-1.10 here. For example, Bauer et al. claim, of their fMRI model, that "[T]his is a system of ordinary differential equations (ODEs) describing the temporal change of the phases $\varphi_1, \ldots, \varphi_r$ of r oscillators, which are coupled by the sine of their phase differences"[52].

In summary, the reader will do well to go through the expressions discussed in this chapter with the aim to understand the physical interpretation, the limitations of the assumptions and possible applications in a variety of fields. The next section deals with the nonlinear formalism.

References

1. Tipler, P. A.; Mosca, G. P., *Physics for Scientists and Engineers*; W.H.Freeman & Co Ltd, 2003.
2. Sands, M.; Feynman, R.; Leighton, R., *The Feynman Lectures on Physics*; Basic Books, 2011.
3. Raman, A., Atomic Force Microscopy. *https://nanohub.org/resources/520* **2014**, *https://www.youtube.com/watch?v=bh9GKXfUs00&list=PLtkeUZItwHK78uGpH76_hhsehADDWnKQB&index=2*.
4. Amo, C. Microscopía De Fuerzas Bimodal Y No Resonante Para Medir Propiedades Físicas Y Químicas a Escala Nanométrica. Universidad Autónoma de Madrid, 2019.
5. MacRae, A. U.; Germer, L. H., Thermal Vibrations of Surface Atoms. *Physical Review Letters* **1962**, *8*, 489-490.
6. Mayants, L. S.; Shaltuper, G. B., General Methods of Analysing Molecular Vibrations. *Journal of Molecular Structure* **1975**, *24*, 409-431.
7. Kučera, O.; Havelka, D.; Cifra, M., Vibrations of Microtubules: Physics That Has Not Met Biology Yet. *Wave Motion* **2017**, *72*, 13-22.
8. Parker, K. J.; Huang, S. R.; Musulin, R. A.; Lerner, R. M., Tissue Response to Mechanical Vibrations for "Sonoelasticity Imaging". *Ultrasound Med Biol* **1990**, *16*, 241-246.
9. Marvi, M.; Ghadiri, M., Retracted Article: A Mathematical Model for Vibration Behavior Analysis of DNA and Using a Resonant Frequency of DNA for Genome Engineering. *Scientific Reports* **2020**, *10*, 3439.
10. Kasas, S.; Ruggeri, F. S.; Benadiba, C.; Maillard, C.; Stupar, P.; Tournu, H.; Dietler, G.; Longo, G., Detecting Nanoscale Vibrations as Signature of Life. *Proceedings of the National Academy of Sciences* **2015**, *112*, 378-381.
11. van der Zee, E. A., The Biology of Vibration. In *Manual of Vibration Exercise and Vibration Therapy*, Rittweger, J., Ed. Springer International Publishing: Cham, 2020; pp 23-38.
12. Mansfield, N. J.; J. Griffin, M., Difference Thresholds for Automobile Seat Vibration. *Applied Ergonomics* **2000**, *31*, 255-261.
13. Blad, M. C.; Christopher Zeeman, E., Oscillations between Repressed Inflation and Keynesian Equilibria Due to Inertia in Decision Making. *Journal of Economic Theory* **1982**, *28*, 165-182.
14. Santos, S.; Gadelrab, K. R.; Souier, T.; Stefancich, M.; Chiesa, M., Quantifying Dissipative Contributions in Nanoscale Interactions. *Nanoscale* **2012**, *4*, 792-800.
15. Graham, K. S., Fundamentals of Mechanical Vibrations. McGraw Hill, Inc: 1993.
16. Steidel, R., *An Introduction to Mechanical Vibrations*, 3 ed.; John Wiley & Sons, 1989.
17. Lozano, J. R.; Garcia, R., Theory of Phase Spectroscopy in Bimodal Atomic Force Microscopy. *Physical Review B* **2009**, *79*, 014110.
18. Butt, H.-J.; Cappella, B.; Kappl, M., Force Measurements with the Atomic Force Microscope: Technique, Interpretation and Applications. *Surface science reports* **2005**, *59*, 1-152.
19. Butt, H.-J.; Jaschke, M., Calculation of Thermal Noise in Atomic I Force Microscopy. *Nanotechnology* **1995**, *6*, 1-7.
20. Gadelrab, K.; Santos, S.; Font, J.; Chiesa, M., Single Cycle and Transient Force Measurements in Dynamic Atomic Force Microscopy. *Nanoscale* **2013**, *5*, 10776-10793.
21. Santos, S.; Gadelrab, K.; Font, J.; Chiesa, M., Single-Cycle Atomic Force Microscope Force Reconstruction: Resolving Time-Dependent Interactions. *New Journal of Physics* **2013**, *15*, 083034.
22. Giessibl, F. J., Forces and Frequency Shifts in Atomic-Resolution Dynamic-Force Microscopy. *Physical Review B* **1997**, *56*, 16010.
23. Anczykowski, B.; Gotsmann, B.; Fuchs, H.; Cleveland, J. P.; Elings, V. B., How to Measure Energy Dissipation in Dynamic Mode Atomic Force Microscopy. *Applied Surface Science* **1999**, *140*, 376-382.
24. Garcia, R.; San Paulo, A., Attractive and Repulsive Tip-Sample Interaction Regimes in Tapping-Mode Atomic Force Microscopy. *Physical Review B* **1999**, *60*, 4961.

25. Santos, S.; Barcons, V.; Verdaguer, A.; Chiesa, M., Subharmonic Excitation in Amplitude Modulation Atomic Force Microscopy in the Presence of Adsorbed Water Layers. *Journal of Applied Physics* **2011**, *110*, 114902.
26. Amadei, C. A.; Tang, T. C.; Chiesa, M.; Santos, S., The Aging of a Surface and the Evolution of Conservative and Dissipative Nanoscale Interactions. *The Journal of Chemical Physics* **2013**, *139*, 084708.
27. Xu, X.; Raman, A., Comparative Dynamics of Magnetically, Acoustically, and Brownian Motion Driven Microcantilevers in Liquids. *Journal of Applied Physics* **2007**, *102*, 034303-034303-8.
28. Melcher, J.; Carrasco, C.; Xu, X.; Carrascosa, J. L.; Gómez-Herrero, J.; de Pablo, P. J.; Raman, A., Origins of Phase Contrast in the Atomic Force Microscope in Liquids. *Proceedings of the National Academy of Sciences* **2009**, *106*, 13655-13660.
29. Hu, S.; Raman, A., Inverting Amplitude and Phase to Reconstruct Tip–Sample Interaction Forces in Tapping Mode Atomic Force Microscopy. *Nanotechnology* **2008**, *19*, 375704.
30. Cleveland, J. P.; Anczykowski, B.; Schmid, A. E.; Elings, V. B., Energy Dissipation in Tapping-Mode Atomic Force Microscopy. *Applied Physics Letters* **1998**, *72*, 2613-2615.
31. Sader, J. E.; Sanelli, J. A.; Adamson, B. D.; Monty, J. P.; Wei, X.; Crawford, S. A.; Friend, J. R.; Marusic, I.; Mulvaney, P.; Bieske, E. J., Spring Constant Calibration of Atomic Force Microscope Cantilevers of Arbitrary Shape. *Review of Scientific Instruments* **2012**, *83*, 103705-103705-16.
32. Proksch, R.; Schäffer, T.; Cleveland, J.; Callahan, R.; Viani, M., Finite Optical Spot Size and Position Corrections in Thermal Spring Constant Calibration. *Nanotechnology* **2004**, *15*, 1344.
33. Morini, G. L., Viscous Dissipation. In *Encyclopedia of Microfluidics and Nanofluidics*, Li, D., Ed. Springer US: Boston, MA, 2008; pp 2155-2164.
34. Stroud, K. A.; Booth, D., *Advanced Engineering Mathematics*; Red Globe Press, 2020.
35. Alshehhi, M.; Alhassan, S. M.; Chiesa, M., Dependence of Surface Aging on DNA Topography Investigated in Attractive Bimodal Atomic Force Microscopy. *Physical Chemistry Chemical Physics* **2017**, *19*, 10231-10236.
36. Santos, S.; Barcons, V.; Christenson, H. K.; Billingsley, D. J.; Bonass, W. A.; Font, J.; Thomson, N. H., Stability, Resolution, and Ultra-Low Wear Amplitude Modulation Atomic Force Microscopy of DNA: Small Amplitude Small Set-Point Imaging. *Applied Physics Letters* **2013**, *103*, 063702-063705.
37. Amadei, C. A.; Yang, R.; Chiesa, M.; Gleason, K. K.; Santos, S., Revealing Amphiphilic Nanodomains of Anti-Biofouling Polymer Coatings. *ACS Applied Materials & Interfaces* **2014**, *6*, 4705-4712.
38. Santos, S.; Olukan, T. A.; Lai, C.-Y.; Chiesa, M., Hydration Dynamics and the Future of Small-Amplitude Afm Imaging in Air. *Molecules (Basel, Switzerland)* **2021**, *26*.
39. Lai, C.-Y.; Santos, S.; Chiesa, M., Systematic Multidimensional Quantification of Nanoscale Systems from Bimodal Atomic Force Microscopy Data. *ACS nano* **2016**, *10*, 6265-6272.
40. Lai, C.-Y.; Olukan, T.; Santos, S.; Al Ghaferi, A.; Chiesa, M., The Power Laws of Nanoscale Forces under Ambient Conditions. *Chemical Communications* **2015**, *51*, 17619-17622.
41. Chiesa, M.; Lai, C.-Y., Surface Aging Investigation by Means of an Afm-Based Methodology and the Evolution of Conservative Nanoscale Interactions. *Physical Chemistry Chemical Physics* **2018**, *20*, 19664-19671.
42. Chiou, Y.-C.; Olukan, T. A.; Almahri, M. A.; Apostoleris, H.; Chiu, C. H.; Lai, C.-Y.; Lu, J.-Y.; Santos, S.; Almansouri, I.; Chiesa, M., Direct Measurement of the Magnitude of the Van Der Waals Interaction of Single and Multilayer Graphene. *Langmuir* **2018**, *34*, 12335-12343.
43. Amadei, C. A.; Lai, C.-Y.; Heskes, D.; Chiesa, M., Time Dependent Wettability of Graphite Upon Ambient Exposure: The Role of Water Adsorption. *The Journal of Chemical Physics* **2014**, *141*, 084709.
44. Lai, C.-Y.; Tang, T.-C.; Amadei, C. A.; Marsden, A. J.; Verdaguer, A.; Wilson, N.; Chiesa, M., A Nanoscopic Approach to Studying Evolution in Graphene Wettability. *Carbon* **2014**, *80*, 784-792.
45. Lai, C.-Y.; Perri, S.; Santos, S.; Garcia, R.; Chiesa, M., Rapid Quantitative Chemical Mapping of Surfaces with Sub-2 Nm Resolution. *Nanoscale* **2016**, *8*, 9688-9694.
46. Eichhorn, A. L.; Dietz, C., Simultaneous Deconvolution of in-Plane and out-of-Plane Forces of Hopg at the Atomic Scale under Ambient Conditions by Multifrequency Atomic Force Microscopy. *Advanced Materials Interfaces* **2021**, *n/a*, 2101288.

47. Santos, S.; Amadei, C. A.; Lai, C.-Y.; Olukan, T.; Lu, J.-Y.; Font, J.; Barcons, V.; Verdaguer, A.; Chiesa, M., Investigating the Ubiquitous Presence of Nanometric Water Films on Surfaces. *The Journal of Physical Chemistry C* **2021**.
48. Wastl, D. S.; Weymouth, A. J.; Giessibl, F. J., Optimizing Atomic Resolution of Force Microscopy in Ambient Conditions. *Physical Review B* **2013**, *87*, 245415.
49. J. Weymouth, A.; Wastl, D.; J. Giessibl, F., Advances in Afm: Seeing Atoms in Ambient Conditions. *e-Journal of Surface Science and Nanotechnology* **2018**, *16*, 351-355.
50. Giessibl, F. J., Advances in Atomic Force Microscopy. *Reviews of modern physics* **2003**, *75*, 949.
51. García, R.; Perez, R., Dynamic Atomic Force Microscopy Methods. *Surface science reports* **2002**, *47*, 197-301.
52. Bauer, L. G.; Hirsch, F.; Jones, C.; Hollander, M.; Grohs, P.; Anand, A.; Plant, C.; Wohlschläger, A., Quantification of Kuramoto Coupling between Intrinsic Brain Networks Applied to Fmri Data in Major Depressive Disorder. *Frontiers in Computational Neuroscience* **2022**, *16*.